To the Graduate Council:

I am submitting herewith a thesis written by Christopher D. Hayes entitled "Initial Developments of a Vibration Model of the Human Head-Neck System." I have examined the final copy of this thesis for form and content and recommend that it be accepted in partial fulfillment of the requirements for the degree of Master of Science, with a major in Engineering Science.

Jack F. Wasserman

Jack F. Wasserman, Major Professor

We have read this thesis
and recommend its acceptance:

Thomas G. Carley

Joseph A. M. Boulet

Accepted for the Council:

C W Minkel

Vice Provost
and Dean of the Graduate School

STATEMENT OF PERMISSION TO USE

In presenting this thesis in partial fulfillment of the requirements for a Master's degree at The University of Tennessee, Knoxville, I agree that the Library shall make it available to borrowers under the rules of the Library. Brief quotations from this thesis are allowable without special permission, provided that accurate acknowledgment of the source is made.

Permission for extensive quotation from or reproduction of this thesis may be granted by my major professor, or in his absence, by the Head of Interlibrary Services when, in the opinion of either, the proposed use of the material is for scholarly purposes. Any copying or use of the material in this thesis for financial gain shall not be allowed without my written permission.

Signature Christopher D. Hayes

Date 5/13/88

INITIAL DEVELOPMENTS OF A VIBRATION MODEL OF THE HUMAN HEAD-NECK SYSTEM

A Thesis

Presented for the

Master of Science Degree

The University of Tennessee, Knoxville

Christopher D. Hayes

June 1988

ACKNOWLEDGMENTS

It would be impossible to individually thank all those who have assisted me with my thesis research and writing, but several have served in key roles. In particular, I would like to thank my major professor, Dr. Jack F. Wasserman, for his great leadership and enduring patience; without his encouragement, this project might never have occurred. I would also like to thank the other members of my committee, Drs. Thomas G. Carley and J. A. M. Boulet, whose advice and criticisms added polish to this text.

Finally, I would like to thank LTC Aaron W. Schopper, CPT Barclay P. Butler, and CPT Roy E. Maday of the United States Army who aided in the research and collection of data for this project; I appreciate your help and the opportunity to work with you.

ABSTRACT

Advances in aviation technology have lead to use of the aviator's helmet as an equipment mounting platform. Military researchers are concerned with the physiological effects and the affect to aviator performance brought about by these changes in helmet design. This thesis deals with the initial developments of a three-dimensional mathematical model which uses representative kinematic equations to describe the effects of changes in helmet weight and center-of-gravity on the human head-neck-helmet system motion in a vibratory environment.

A four degree of freedom mathematical model was developed consisting of a two pivot description connected by a system of rotational springs. The equations of motion were derived using Lagrange's equation, producing four second order, nonlinear differential equations with nonconstant coefficients. The equations were linearized by neglecting high order terms and assuming small angles.

A computer program was used to evaluate the linearized θ_H equation and to compare results to experimental physical data. The results showed that the θ_H equation reproduced the frequency responses exhibited in the physical data. Interpretation of these results was used to speculate about mechanisms governing muscle reactions due to certain loading conditions.

TABLE OF CONTENTS

LIST OF TABLES

LIST OF FIGURES

FIGURE PAGE

NOMENCLATURE

θ_N, θ_H = Neck, Head rotations about y axis

ϕ_N, ϕ_H = Neck, Head rotations about z axis

θ_{NO}, θ_{HO} = Initial angular deflections about y axis

ϕ_{NO}, ϕ_{HO} = Initial angular deflections about z axis

Θ_N, Θ_H = $\theta_N + \theta_{NO}$, $\theta_H + \theta_{HO}$

Φ_N, Φ_H = $\phi_N + \phi_{NO}$, $\phi_H + \phi_{HO}$

l_N = Length of neck rod to neck mass

L_N = Length of neck rod

L_H = Length of head rod

m_N = Mass of neck

m_H = Mass of head/helmet

I_{ij}^K = Inertia terms of head/helmet

K: rotation location

i, j: axes

β_c = rotational spring stiffnesses

c: θ_N, θ_H, ϕ_N, ϕ_H

x, y, z = directions of excitations

I. INTRODUCTION

As advances are being made in aviation technology, designers have begun to use the aviator's helmet as an equipment mounting platform. Equipment which enhances night vision, provides flight parameter displays, and allows integrated head/weapon tracking has been attached to various locations on the aviator's helmet. These attachments have significantly increased helmet weight, changed the center-of-gravity (CG), and therefore altered the inertial properties of the helmet. How these changes in weight and CG affect pilot performance is a major concern of military researchers. This thesis deals with the initial developments of a three-dimensional mathematical model which uses representative kinematic equations to describe the effects of changes in helmet weight and CG on the head-neck-helmet system motion in a vibratory environment.

Literature Review

Early mathematical models developed to describe head-neck response were mainly concerned with motion due to impact or high acceleration/deceleration events, as in automobile crash simulations. A study performed by Ewing and Thomas (1972) has been the basis for several such models. In this study, a number of military subjects were instrumented with accelerometer packages to measure head and neck motion during sled acceleration tests. The accelerometers measured the accelerations achieved by the head and neck for sled accelerations up to fifteen times the gravitational acceleration of earth (15 G's), while high speed photography documented head-neck angles and displacements.

A model proposed by Frisch and Cooper (1978), using data from the sled acceleration experiments, consisted of two pivot points representing the rotations of the head and neck in the mid-sagittal plane (the anatomical plane that splits the body in equal left and right halves from head to toe). The lower pivot point was located at the first thoracic vertebral body (T1) at the base of the neck. Two locations were proposed for the upper pivot: the occipital condyles, a point located at the junction of the first cervical vertebral body (C1) and the base of the skull, and a point, determined through data analysis, that lies slightly above the CG of the head, located just forward and above the ear canal. The analysis involved head-neck motion data of nine subjects undergoing sled accelerations of 8.1 to 15.1 G's.

The model was consistent with the physical data, and provided new insights to head-neck muscle mechanisms. The neck deceleration measured at T1 seemed to be propagated to the head through the cervical spine; the level of acceleration influenced the range of motion. The analysis also showed that use of the proposed pivot at the occipital condyles produced greater discrepancies than the use of the pivot above the head CG. These discrepancies may have been due to the fact that the physical data indicate translation as well as rotation at the occipital condyles (a condition not described in the model at that point). Conversely, the proposed alternate pivot produced a mathematically defined pure rotation for the model that was consistent with the physical data.

Another model was developed by Schneider and Bowman (1978) also using data from the Ewing and Thomas study. Sled acceleration data from five subjects undergoing 6 to 15 G accelerations was used to test the model. Their model, a whole body model, consisted of nine body segments and eight pivot locations, with particular attention focused on movement of the head and neck. A two pivot model was again proposed, with the lower pivot representing T1 and the upper pivot at the occipital condyles. A series of linear springs and spring-damper systems was used to approximate the stiffness and the damping properties of the muscles in the neck. Muscle tension parameters in the model were varied, and the results compared to the sled acceleration data. The comparison seemed to indicate that even if a subject could anticipate the impending acceleration, the neck muscles could not fully counteract the motion. The results also indicated that the primary mechanisms generating the head angular accelerations were the overall sled kinematics and body configuration present during the acceleration profile.

In a third study utilizing the same sled acceleration data, Smith and Anderson (1978) considered the frequency characteristics of the motion. Data from six subjects experiencing 6 to 11 G accelerations were used to compute frequency information from the Fourier transform of the time domain information. This was accomplished by using a technique similar to impact testing, i.e. measuring the force input and the subsequent response, and collecting time averaged data of 24 runs per each subject to produce the frequency response. Of particular interest were the resonances found at 6, 17, and 30 Hz. The 6 Hz frequency seemed to be associated with the period of complete head motion, the 17 Hz response corresponded to the head rebound after achieving its lowest position, and the 30 Hz resonance possibly indicated a nonlinear interaction during the head rebound. From this data, an empirical model was designed to predict the head response due to measured neck acceleration. The model performed satisfactorily, and had advantages over purely mathematical models because its development was based on observed inertial responses.

The previously mentioned studies provided significant gains in the understanding of mechanisms of the head and neck undergoing high-G accelerations, but they did not address the problem typically experienced by military aviators, which is long term exposure to low level vibration. In addition, it is important to understand the frequency responses during this type of exposure which could have some effect on pilot performance. Two studies, performed by Viviani and Berthoz (1975) and by Jex and Magdaleno (1978), touch on this subject.

The Viviani and Berthoz study used small amplitude, sinusoidal and impulsive forces of up to 15N to excite the head and neck of three subjects. The experimental design consisted of tests which applied the forces to the top of the head with a rod/shaker assembly and measuring the linear displacement of the head. An analytical model was conceived utilizing two massless rods and two pivot points to simulate the rotational motion in the mid-sagittal plane. The pivot points were located at the junction of the sixth and the seventh cervical vertebral bodies and at the atlano-occipital articulation (at the same location as the occipital condyles). Representations of rotational springs were used at the pivot points to add stiffness to the system and to model muscular functions. From the comparison of experimental data and model performance, several conclusions were made. Above 2 Hz, the head-neck system exhibited linear responses to the sinusoidal forcing function up to the tested maximum of 20

Hz. Some nonlinearities observed in this frequency range were thought to be caused by the viscoelastic, or time-dependent stiffness/damping, properties of the neck muscles. The investigation supported the use of two points of rotation for modeling purposes.

Jex and Magdaleno proposed and developed a whole body vibration feedthrough model to predict the effect of vibration on the head and hands, and thus performance, of the semisupine pilot. The model was validated using data from a series of tracking experiments during whole body vibration. This two-dimensional model exhibited the same characteristic head bobbing motion in the 4-6 Hz range as the experimental data. In the comparisons of the model and physical data, various seating positions and control stick impedances were evaluated for changes in pilot tracking performance.

Although these last two studies dealt with vibratory forces, they still did not address several important factors in determining the effects of helmet weight and CG on aviator performance. Viviani and Berthoz's approach did not present an appropriate mode of excitation, since a pilot is shaken through his seat and not by direct connection to the head. While Jex and Magdaleno used the appropriate excitation to study the performance of the pilot, they did not specifically address the problem of various loads on the head-neck system; nor does the two-dimensional nature of the model allow the full range of analysis concerning changes in helmet design. To understand the effects of helmet design changes, coupled with vibratory excitation, on the performance of military aviators requires the development of a three-dimensional, predictive model of the head-neck-helmet system which addresses all of these factors.

Proposed Model

Initial steps in the development of such a three-dimensional, predictive model were the main thrust of this investigation. These steps included the formulation of the kinematic equations governing a proposed system, the development of some form of computer implementation, and the validation of the model by comparison with experimental data.

The proposed analytical model was a two pivot system much like that used in the past studies. Simply, a lower pivot represented the junction between the chest and neck, while an upper pivot modeled the connection between the neck and head. The representative masses of the neck, head, and helmet were connected by a system of massless rods to allow energy transfer while maintaining constant separations. Mathematical formulations representing rotational springs limited the head-neck motion and attempted to return the system to its equilibrium position.

The equations of motion for the system were developed using the Lagrange formulation of the system energy in generalized coordinates.

Because the initial equations of motion were nonlinear, and thus difficult to solve by hand, a procedure for simplification was devised. By assuming small amplitude solutions, the system of equations was reduced to a linear system. Then, a sinusoidal forcing function and its corresponding response were specified, further reducing the complexity of the system. A computer program was used to evaluate the system for various physical parameters.

The physical parameters used in the evaluation of the model corresponded to those conditions used by Maday and Butler (1985) at the U.S. Army Aeromedical Research Laboratory, Fort Rucker, Alabama. These researchers tested physical reactions, such as muscle fatigue and tracking performance, of six military personnel to changes in helmet design. Each subject performed tracking tasks during single- and multi-axis random excitation while wearing a variable weight/CG helmet. Vibration data from this tracking investigation was used for validation of the proposed computer model.

II. MODEL EQUATION FORMULATION

The development of the equations of motion governing the three-dimensional model required several steps. First, a physical description of the model and its corresponding anatomical representations were produced. This step included the description of the coordinate systems and the naming of the physical parameters. Then, the nonlinear equations of motion were derived using Lagrange's equation. Finally, a linearization procedure was performed to aid in the solution of the equation system.

System Representation

The purpose of the model design was to describe mathematically the anatomical configurations and muscle mechanisms of the human head-neck system during vibratory excitation in three orthogonal directions (directions at right angles to each other). Also, the additional mass and center-of-gravity (CG) of a helmet was to be considered to test the effects of changes in helmet design. Thus a system of pivots, rotational springs, point masses, and inextensible massless rods placed in a moving coordinate frame was used to devise the model structure.

A two-pivot formulation (shown in Figure 1) was chosen to represent the head-neck system. The pivots represent the flexion and extension (forward and backward

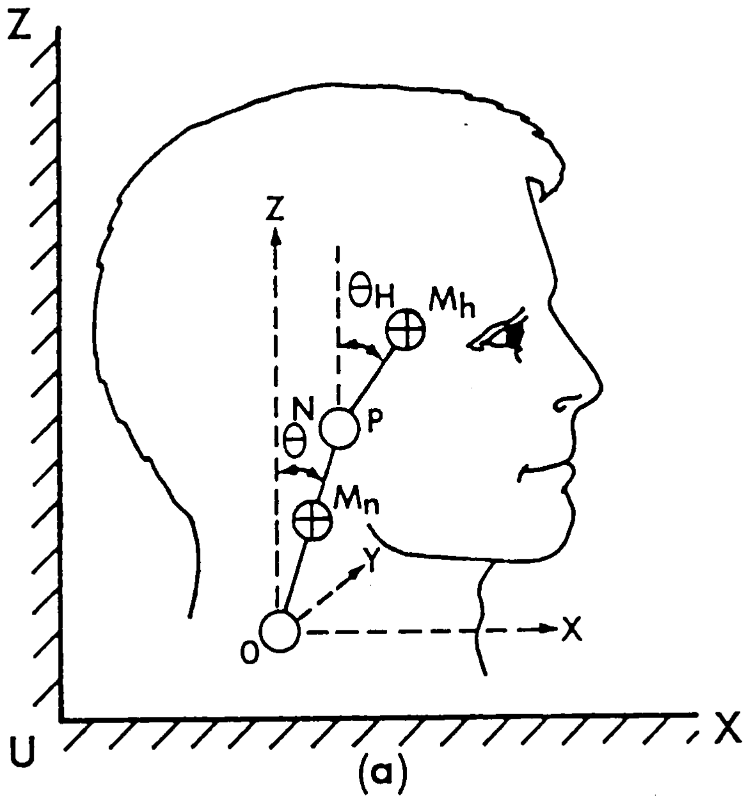

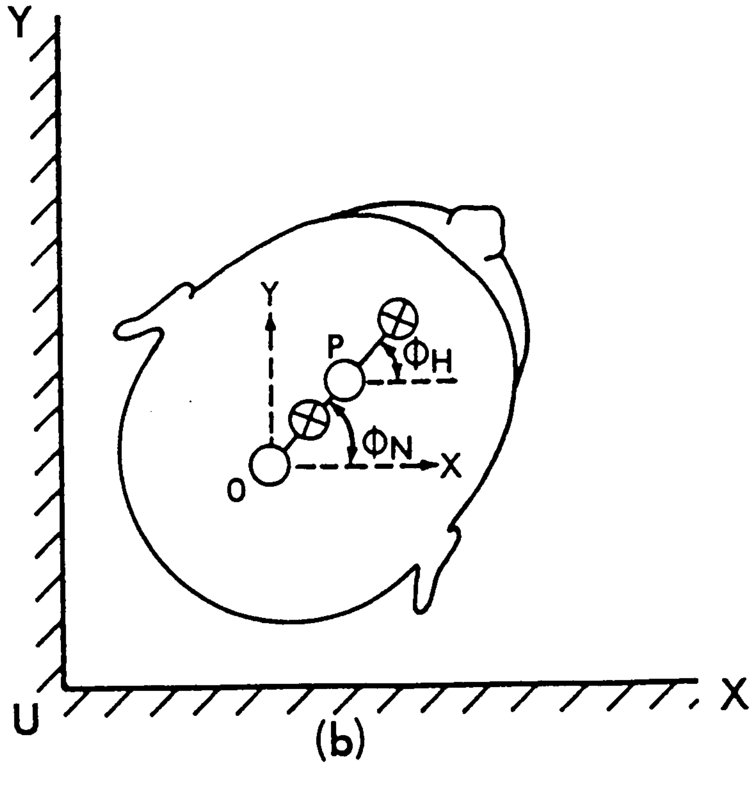

Figure 1. Four Degree of Freedom System with Inertial Frame Located at Point U and Moving Frame Located at Point O: (a) Side View; (b) Top View.

rotation in the mid-sagittal plane) and the transverse (left to right rotation) motions of the head and neck. For simplicity, lateral motion (side to side rotation) was not considered in this development. This two-pivot system was placed in a moving coordinate frame with its origin at O. An inertial, or stationary, coordinate frame with its origin at **U** was used to define the absolute displacement of the moving frame in the x, y, and z directions.

The lower pivot, representing the junction of the seventh cervical and first thoracic vertebrae of the neck, was placed at O in the moving coordinate frame. This pivot provided a rotation in the mid-sagittal plane (θ_N) and a rotation in the transverse plane (ϕ_N). The upper pivot **P** represented the position where rotations of the head-neck junction occurs. The exact position of **P** was left as a variable that depends on specified head-neck geometry (the occipital condyles are commonly used as the anatomical reference point). This pivot also allowed rotations in the mid-sagittal plane (θ_H) and in the transverse plane (ϕ_H). The measures of these angles were all determined from the direction-fixed axes of the moving coordinate frame.

Two point masses were used in the model description. The lower point mass, m_N, represented the mass of the neck, while the upper point mass, m_H, represented the combined mass of the head and helmet. The combined mass could be used safely in this analysis since Wasserman (1984) showed that the variable weight/CG helmet used in the experimental analysis exhibited resonant frequencies above the range being tested in this investigation (i.e., above 30 hz). In addition, the upper point mass carried the inertial properties for the combined head-helmet structure. The inertial element for the neck were assumed to be negligible in comparison to those of the head-helmet, and thus these properties for the neck were set to zero.

The distances between the two pivots and the distance from pivot P to the CG of the combined head-helmet mass were maintained by inextensible, massless rods. These rods were theoretical entities which had no mass, maintained fixed distances, and provided a medium for motion or energy transfer. To allow changes in the head-neck-helmet geometry, the lengths of these rods were left as variables to be specified. The neck mass was attached to the lower rod at a specified distance (l_N), while the head-helmet mass was placed at the end of the upper rod (a distance of L_H). The lower rod maintained a length of L_N.

The four rotations (θ_N, θ_H, ϕ_N, ϕ_H) were each constrained by a rotational spring that stiffened proportionally to the angle of deflection. The $\beta_{\theta N}$ and $\beta_{\theta H}$ springs limited the flexion-extension motion of the head and neck, while the $\beta_{\phi N}$ and $\beta_{\phi H}$ springs limited the left to right rotation. These springs approximated the function of the primary muscle groups represented in Table 1.

TABLE 1

PARAMETER REPRESENTATIONS OF MUSCLE GROUPS

BODY SEGMENT	MUSCLES	ACTION	MODEL PARAMETER	SPRING NOTATION
NECK	STERNOCLEIDOMASTOID, SCALENI, LONGUS CERVICIS, LONGUS CAPITIS	FLEXION	θ_N	$\beta_{\theta N}$
	SPLENIUS CERVICIS, SEMISPLINALIS CERVICIS, ILIOCOSTALIS CERVICIS, INTERSPINALIS, MULTIFIDUS, ROTATORS	EXTENSION	θ_N	$\beta_{\theta N}$
	RT. SPLENIUS CERVIS, RT. LONGISSIMUS CERVICIS, RT. ILIOCOSTALIS CERVICIS, RT. and LT. LONGUS COLLI, LT. SEMISPLINALIS CERVICIS, LT. ROTATORS, LT. SCALENI,	ROTATION to the right	ϕ_N	$\beta_{\phi N}$
	SAME MUSCLES ON OPPOSITE SIDE	ROTATION to the left	ϕ_N	$\beta_{\phi N}$
HEAD	LONGUS CAPITUS, RECTUS CAPITIS ANTERIOR, STERNOCLEIDOMASTOID	FLEXION	θ_H	$\beta_{\theta H}$
	SPLENIUS CAPITIS, SEMI-SPINALIS CAPITIS, OBLIQUUS CAPITIS SUPERIOR, RECTUS CAPITIS POSTERIOR MAJOR and MINOR	EXTENSION	θ_H	$\beta_{\theta H}$
	LT. STERNOCLEIDOMASTOID, RT. SPLENIUS CAPITIS, RT. LONGISSIMUS CAPITIS, RT. OBLIQUUS CAPITIS INFERIOR, RT. RECTUS CAPITIS POSTERIOR MINOR	ROTATION to the right	ϕ_H	$\beta_{\phi H}$
	SAME MUSCLES ON OPPOSITE SIDE	ROTATION to the left	ϕ_H	$\beta_{\phi H}$

No damping or energy absorption factor was included in the rotational constraints for this initial model. This allowed the constituent equations to be more readily simplified, although they would not theoretically model the reactions of human muscles as closely as if damping were included. But accurately quantifying such damping factors for muscle is, at best, an inexact effort with today's present technology; exclusion of these values does not hinder the overall approach rendered by this model.

After formulation of the basic structure of the model, the vibration excitations or forcing functions were the last components of the model to be described. These vibration inputs were left for specification during the solution of the equation system, but the basic form expresses the displacement of the moving coordinate frame in relationship to the inertial frame. The position of the moving frame at any time t was expressed as the sum of the initial position and the time-dependent displacement or excitation. For example, the position $(X,Y,Z)_o$ of point O at any time t is

$$(X)_o = (X_o)_o + x(t)$$

$$(Y)_o = (Y_o)_o + y(t)$$

$$(Z)_o = (Z_o)_o + z(t)$$

where $(X_o, Y_o, Z_o)_o$ is the initial location of point O, and

$x(t)$, $y(t)$, $z(t)$ are expressions for the time displacements of the coordinate frame due to an excitation.

In a similar fashion, the exact position of the masses and pivots could be determined at any time t in relation to the point O. For example, the position $(x,y,z)_H$ of the head-helmet mass at any time t could be expressed as

$$x_H = L_N \sin\theta_N \cos\Phi_N + L_H \sin\theta_H \cos\Phi_H$$

$$y_H = L_N \sin\theta_N \sin\Phi_N + L_H \cos\theta_H \cos\Phi_H$$

$$z_H = L_N \cos\theta_N + L_H \cos\theta_H$$

where θ_N, θ_H, Φ_N, and Φ_H represent the measured deflections from the defined axes for θ_N, θ_H, ϕ_N, and ϕ_H, respectively.

The position of any point in the model could be expressed in relation to the inertial frame U by combining these two ideas. The position of the head-helmet mass in relation to the inertial frame is

$$X_H = (X)_O + x_H$$

$$Y_H = (Y)_O + y_H$$

$$Z_H = (Z)_O + z_H$$

where $(X, Y, Z)_O$ and $(x,y,z)_H$ were previously defined.

Notice that in these descriptions each position was represented by the length of a rod multiplied by some trigonometric functions of the angles of deflection, plus the displacement from the inertial system. Since the lengths of the rods were constant once they were specified, and the displacement of the moving coordinate system was prescribed, then the deflections of the system could be described with the four rotations. Therefore, the mathematical model was considered to have four degrees of freedom: θ_N, θ_H, ϕ_N, and ϕ_H. This type of representation in a moving coordinate frame allowed the system to be considered nonconservative.

Derivation of Equations of Motion

With the generalized coordinates within the inertial and moving coordinate frames defined, the next step in the development of the model was the formulation of the equations governing the system. Because of the nature of the physical description, an excellent method for deriving these equations was the use of an energy formulation. Lagrange's equation using generalized coordinates was chosen as the method for the formulation of the equation system.

In its most general form for a conservative system, Lagrange's equation is

$$\frac{d}{dt}\left[\frac{\delta \pounds}{\delta \dot{q}_i}\right] - \frac{\delta \pounds}{\delta q_i} = 0$$

where $\pounds = T - V$,

T is the system kinetic energy,

V is the system potential energy,

q_i represents the generalized coordinates for the system.

As mentioned previously, the physical description of the model characterized the system as nonconservative, due to the moving coordinate frame at O. This would seem to preclude the use of the above form of Lagrange's equation. A closer examination shows that the excitation at O did not act directly through any mass, thus not contributing directly to any generalized force. This condition allowed the use of Lagrange's equation as shown (Greenwood, 1965).

With the selection of this form of Lagrange's equation completed, each term of the Lagrange functional $\pounds$ was to be determined. The system kinetic energy T was formulated from the velocities achieved by the masses. The general form for the equation for T is

$$T = \frac{1}{2} \left(\Sigma\, m_i\, v_i^2 + \Sigma\, I\, \Omega^2 \right)$$

where m_i represents the individual masses,

v_i represents the individual velocities,

I represents the mass moment of inertia for the system,

Ω represents the angular velocity.

The velocity for each mass was derived from the first derivative of the position vector for that mass. For example, the velocity vector for the combined head-helmet mass was

$$\vec{v}_H = \dot{X}_H \,\hat{i} + \dot{Y}_H \,\hat{j} + \dot{Z}_H \,\hat{k}$$

where

$$\dot{X}_H = (\dot{X})_o + \dot{x}_H$$

$$\dot{Y}_H = (\dot{Y})_o + \dot{y}_H$$

$$\dot{Z}_H = (\dot{Z})_o + \dot{z}_H$$

and where

$$(\dot{X})_o = \dot{x}(t)$$

$$\dot{x}_H = L_N\dot{\theta}_N \cos\theta_N \cos\Phi_N - L_N\dot{\Phi}_N \sin\theta_N \sin\Phi_N + L_H\dot{\theta}_H \cos\theta_H \cos\Phi_H - L_H\dot{\Phi}_H \sin\theta_H \sin\Phi_H$$

$$(\dot{Y})_o = \dot{y}(t)$$

$$\dot{y}_H = L_N\dot{\theta}_N \sin\Phi_N + L_N\dot{\Phi}_N \sin\theta_N \cos\Phi_N + L_H\dot{\theta}_H \cos\theta_H \sin\Phi_H - L_H\dot{\Phi}_H \sin\theta_H \cos\Phi_H$$

$$(\dot{Z})_o = \dot{z}(t)$$

$$\dot{z}_H = - L_N\dot{\theta}_N \sin\theta_N - L_H\dot{\theta}_H \sin\theta_H$$

Collecting these terms and calculating v_H^2 for the kinetic energy equation yielded

$$v_H^2 = \dot{x}^2 + \dot{y}^2 + \dot{z}^2 + 2\, L_N\dot{\theta}_N \,[\cos\theta_N \,(\dot{x} \cos\Phi_N + \dot{y} \sin\Phi_N) - \dot{z} \sin\theta_N]$$

$$+ 2\, L_N\dot{\Phi}_N\, [\sin\Theta_N\, (-\dot{x}\, \sin\Phi_N + \dot{y}\, \cos\Phi_N)]$$

$$+ 2\, L_H\dot{\Theta}_H\, [\cos\Theta_H\, (\dot{x}\, \cos\Phi_H + \dot{y}\, \sin\Phi_H) - \dot{z}\, \sin\Theta_H]$$

$$+ 2\, L_H\dot{\Phi}_H\, [\sin\Theta_H\, (-\dot{x}\, \sin\Phi_H + \dot{y}\, \cos\Phi_H)]$$

$$+ L_N{}^2\dot{\Theta}_N{}^2 + 2\, L_N L_H\dot{\Theta}_N\dot{\Theta}_H\, \cos\Theta_N\, \cos\Theta_H\, \cos(\Phi_N - \Phi_H)$$

$$+ L_N{}^2\dot{\Phi}_N{}^2\sin^2\Theta_N + 2\, L_N L_H\dot{\Theta}_N\dot{\Phi}_H\, \cos\Theta_N\, \sin\Theta_H\, \sin(\Phi_N - \Phi_H)$$

$$+ 2\, L_N L_H\dot{\Phi}_N\dot{\Theta}_H\, \sin\Theta_N\, \cos\Theta_H\, \sin(\Phi_N - \Phi_H)$$

$$+ 2\, L_N L_H\dot{\Phi}_N\dot{\Phi}_H\, \sin\Theta_N\, \sin\Theta_H\, \cos(\Phi_N - \Phi_H) + L_H{}^2\dot{\Theta}_H{}^2$$

$$+ 2\, L_N L_H\dot{\Theta}_N\dot{\Theta}_H\, \sin\Theta_N\, \sin\Theta_H + L_H{}^2\dot{\Phi}_H{}^2\, \sin^2\Theta_H$$

Terms for $v_N{}^2$ were collected in the same manner.

The inertia terms for the head-helmet mass were calculated with respect to the pivots O and P and to the motion about the pivots. Symbolically,

$$[I]\,\{\Omega\}^2 = I_{yy}{}^O\, \dot{\Theta}_N{}^2 - 2\, I_{yz}{}^O\, \dot{\Theta}_N\dot{\Phi}_N + I_{zz}{}^O\, \dot{\Phi}_N{}^2$$
$$+ I_{yy}{}^P\, \dot{\Theta}_H{}^2 - 2\, I_{yz}{}^P\, \dot{\Theta}_H\dot{\Phi}_H + I_{zz}{}^P\, \dot{\Phi}_H{}^2$$

After the collection of these terms and the terms for the velocities, the kinetic energy **T** was calculated using the general form

$$T = \tfrac{1}{2}\, m_N\, v_N{}^2 + \tfrac{1}{2}\, m_H\, v_H{}^2 + \tfrac{1}{2}\, [I]\, \{\Omega\}^2$$

The resulting equation is represented in Table 2.

The system potential energy was calculated from the sum of the spring potential energy and the gravitational potential energy. The general equation for the spring potential energy for rotational springs was

TABLE 2

MODEL SYSTEM ENERGY EQUATIONS

Kinetic Energy:

$$
\begin{aligned}
T = {} & \tfrac{1}{2}\,(m_N + m_H)\,(\dot{x}^2 + \dot{y}^2 + \dot{z}^2) \\
& + (m_N l_N + m_H L_H)\,\dot{\Theta}_N\,[\cos\Theta_N\,(\dot{x}\cos\Phi_N + \dot{y}\sin\Phi_N) - \dot{z}\sin\Theta_N] \\
& + (m_N l_N + m_H L_N)\dot{\Phi}_N\,[\sin\Theta_N\,(-\dot{x}\sin\Phi_N + \dot{y}\cos\Phi_N)] \\
& + \tfrac{1}{2}\,(m_N l_N{}^2 + m_H L_N{}^2)\,(\dot{\Theta}_N{}^2 + \dot{\Phi}_N{}^2\sin^2\Theta_N) \\
& + m_H L_H \dot{\Theta}_H\,[\cos\Theta_H\,(\dot{x}\cos\Phi_H + \dot{y}\sin\Phi_H) - \dot{z}\sin\Theta_H] \\
& + m_H L_H \dot{\Phi}_H\,[\sin\Theta_H\,(-\dot{x}\sin\Phi_H + \dot{y}\cos\Phi_H)] \\
& + m_H L_N L_H\,[\dot{\Theta}_N\dot{\Theta}_H\cos\Theta_N\cos\Theta_H\cos(\Phi_N - \Phi_H) \\
& \qquad + \dot{\Phi}_N\dot{\Theta}_H\sin\Theta_N\cos\Theta_H\sin(\Phi_N - \Phi_H)] \\
& \quad + m_H L_N L_H\,[\dot{\Theta}_N\dot{\Phi}_H\cos\Theta_N\sin\Theta_H\cos(\Phi_N - \Phi_H) \\
& \qquad\qquad + \dot{\Phi}_N\dot{\Phi}_H\sin\Theta_N\sin\Theta_H\cos(\Phi_N - \Phi_H) \\
& \qquad\qquad + \dot{\Theta}_N\dot{\Theta}_H\sin\Theta_N\sin\Theta_H] \\
& \quad + \tfrac{1}{2}\,m_H L_H{}^2\,(\dot{\Theta}_H{}^2 + \dot{\Phi}_H{}^2\sin^2\Theta_H) \\
& \quad + \tfrac{1}{2}\,(I_{yy}{}^{O}\,\dot{\Theta}_N{}^2 - 2\,I_{yz}{}^{O}\,\dot{\Theta}_N\dot{\Phi}_N + I_{zz}{}^{O}\,\dot{\Phi}_N{}^2) \\
& \quad + \tfrac{1}{2}\,(I_{yy}{}^{P}\,\dot{\Theta}_H{}^2 - 2\,I_{yz}{}^{P}\,\dot{\Theta}_H\dot{\Phi}_H + I_{zz}{}^{P}\,\dot{\Phi}_H{}^2)
\end{aligned}
$$

Potential Energy:

$$
\begin{aligned}
V = {} & \tfrac{1}{2}\,\beta_{\Theta N}\,\Theta_N{}^2 + \tfrac{1}{2}\,\beta_{\Theta H}\,(\Theta_H - \Theta_N)^2 + \tfrac{1}{2}\,\beta_{\Phi N}\,\Phi_N{}^2 \\
& + \tfrac{1}{2}\,\beta_{\Phi H}\,(\Phi_H - \Phi_N)^2 + m_N\,g\,l_N\cos\Theta_N \\
& + m_H\,g\,(L_N\cos\Theta_N + L_H\cos\Theta_H) + (m_H + m_N)\,g\,z_o
\end{aligned}
$$

$$V_s = \frac{1}{2} \Sigma \, k_i \, \alpha_i$$

where k_i is the stiffness of the spring,

α_i is the angle of deflection.

From this general form, the spring potential energy for the model was

$$V_s = \frac{1}{2} \, \beta_{\theta N} \, \theta_N^2 + \frac{1}{2} \, \beta_{\theta H} \, (\theta_H - \theta_N)^2$$
$$+ \frac{1}{2} \, \beta_{\Phi N} \, \Phi_N^2 + \frac{1}{2} \, \beta_{\Phi H} \, (\Phi_H - \Phi_N)^2$$

The general form of the gravitational potential energy is

$$V_G = \Sigma \, m_i h_i g$$

where m_i is the individual mass,

h_i is the mass's height above the moving coordinate system,

g is the gravitational constant.

From this form, the gravitational potential energy for the system was

$$V_G = m_N \, g \, l_N \cos\theta_N + m_H \, g \, (L_N \cos\theta_N + L_H \cos\theta_H)$$
$$+ (m_H + m_N) \, g \, z_O$$

These potential energy expressions were collected in a single equation expressing the system potential energy. This equation is also presented in Table 2.

From the kinetic energy and potential energy equations, the Lagrangian functional was formed as

$$
\begin{aligned}
\pounds = {} & \tfrac{1}{2}\,(m_N + m_H)\,(\dot{x}^2 + \dot{y}^2 + \dot{z}^2) \\
& + (m_N l_N + m_H L_N)\,\dot{\theta}_N\,[\cos\theta_N\,(\dot{x}\cos\Phi_N + \dot{y}\sin\Phi_N) - \dot{z}\sin\theta_N] \\
& + (m_N l_N + m_H L_N)\dot{\Phi}_N\,[\sin\theta_N\,(-\dot{x}\sin\Phi_N + \dot{y}\cos\Phi_N)] \\
& + \tfrac{1}{2}\,(m_N l_N^2 + m_H L_N^2)\,(\dot{\theta}_N^2 + \dot{\Phi}_N^2\sin^2\theta_N) \\
& + m_H L_H\dot{\theta}_H\,[\cos\theta_H\,(\dot{x}\cos\Phi_H + \dot{y}\sin\Phi_H) - \dot{z}\sin\theta_H] \\
& + m_H L_H\dot{\Phi}_H\,[\sin\theta_H\,(-\dot{x}\sin\Phi_H + \dot{y}\cos\Phi_H)] \\
& + m_H L_N L_H\,[\dot{\theta}_N\dot{\theta}_H\cos\theta_N\cos\theta_H\cos(\Phi_N - \Phi_H) \\
& \qquad + \dot{\Phi}_N\dot{\theta}_H\sin\theta_N\cos\theta_H\sin(\Phi_N - \Phi_H)] \\
& + m_H L_N L_H\,[\dot{\theta}_N\dot{\Phi}_H\cos\theta_N\sin\theta_H\cos(\Phi_N - \Phi_H) \\
& \qquad + \dot{\Phi}_N\dot{\Phi}_H\sin\theta_N\sin\theta_H\cos(\Phi_N - \Phi_H) \\
& \qquad\qquad + \dot{\theta}_N\dot{\theta}_H\sin\theta_N\sin\theta_H] \\
& + \tfrac{1}{2}\,m_H L_H^2\,(\dot{\theta}_H^2 + \dot{\Phi}_H^2\sin^2\theta_H) \\
& + \tfrac{1}{2}\,(I_{yy}^{O}\,\dot{\theta}_N^2 - 2\,I_{yz}^{O}\,\dot{\theta}_N\dot{\Phi}_N + I_{zz}^{O}\,\dot{\Phi}_N^2) \\
& + \tfrac{1}{2}\,(I_{yy}^{P}\,\dot{\theta}_H^2 - 2\,I_{yz}^{P}\,\dot{\theta}_H\dot{\Phi}_H + I_{zz}^{P}\,\dot{\Phi}_H^2) \\
& - \tfrac{1}{2}\,\beta_{\theta N}\,\theta_N^2 - \tfrac{1}{2}\,\beta_{\theta H}\,(\theta_H - \theta_N)^2 - \tfrac{1}{2}\,\beta_{\Phi N}\,\Phi_N^2 \\
& - \tfrac{1}{2}\,\beta_{\Phi H}\,(\Phi_H - \Phi_N)^2 - m_N\,g\,l_N\cos\theta_N \\
& - m_H\,g\,(L_N\cos\theta_N + L_H\cos\theta_H) - (m_H + m_N)\,g\,z_O
\end{aligned}
$$

Then, using Lagrange's equation, the equations of motion were calculated for the four generalized coordinates. In a symbolic matrix form, the equations appear as

$$[M]\{\ddot{q}_i\} + [R]\{\dot{q}_i^2\} + [K]\{q_i\} + mL\{A\} = \{0\}$$

where $[M]$ is the mass matrix,

$[R]$ contains terms relating to Coriolis forces,

$[K]$ is the stiffness matrix,

$mL\{A\}$ are terms expressing the specified excitation.

The resulting system of four equations of motion are presented in Table 3. The detailed steps for the formulation of the equations are presented in Appendix A.

These four equations were recognized as second order, nonlinear differential equations with nonconstant coefficients. Because of the complexity of these equations, analytical solutions do not exist. Hence, some degree of simplification was desired before any solution was attempted.

Linearization of Equation Set

The nonlinear nature of the set represented a number of terms which may simultaneously vary within the system. In an initial development, the key to evaluating and shaping a model is being able to understand the solution and identify prevailing trends. Thus, a linearization

TABLE 3

NONLINEAR EQUATIONS OF MOTION

$$
\begin{aligned}
\theta_N :\ & (m_N l_N^2 + m_H L_N^2 + I_{yy}^O)\ddot{\theta}_N - I_{yz}^O\ddot{\phi}_N + \{m_H L_N L_H\,[\cos\theta_N\cos\theta_H\cos(\phi_N-\phi_H) + \sin\theta_N\sin\theta_H]\}\ddot{\theta}_H \\
& + [m_H L_N L_H\,\cos\theta_N\sin\theta_H\sin(\phi_N-\phi_H)]\ddot{\phi}_H - [(m_N l_N^2 + m_H L_N^2)\,\cos\theta_N\sin\theta_N]\dot{\phi}_N^2 \\
& - [2\, m_H L_N L_H\,\cos\theta_N\cos\theta_H\sin(\phi_N-\phi_H)]\dot{\theta}_H\dot{\phi}_N + [2\, m_H L_N L_H\,\cos\theta_N\cos\theta_H\sin(\phi_N-\phi_H)]\dot{\theta}_H\dot{\phi}_H \\
& + \{m_H L_N L_H\,[-\cos\theta_N\sin\theta_H\cos(\phi_N-\phi_H) + \sin\theta_N\cos\theta_H]\}\dot{\theta}_H^2 - [m_H L_N L_H\,\cos\theta_N\sin\theta_H\cos(\phi_N-\phi_H)]\dot{\phi}_H^2 \\
& + (\beta_{\theta N} + \beta_{\theta H})\theta_N - \beta_{\theta H}\theta_H + (m_N l_N + m_H L_N)\,[\,\ddot{x}\,\cos\theta_N\cos\phi_N + \ddot{y}\,\cos\theta_N\sin\phi_N - (\ddot{z} + g)\sin\theta_N] = 0
\end{aligned}
$$

$$
\begin{aligned}
\phi_N :\ & - I_{yz}^O\ddot{\theta}_N + [(m_N l_N^2 + m_H L_N^2)\sin^2\theta_N + I_{zz}^O]\ddot{\phi}_N + [m_H L_N L_H\,\sin\theta_N\cos\theta_H\sin(\phi_N-\phi_H)]\ddot{\theta}_H \\
& + [m_H L_N L_H\,\sin\theta_N\sin\theta_H\cos(\phi_N-\phi_H)]\ddot{\phi}_H + [2\,(m_N l_N^2 + m_H L_N^2)\,\sin\theta_N\cos\theta_N]\dot{\theta}_N\dot{\phi}_N \\
& - [m_H L_N L_H\,\sin\theta_N\sin\theta_H\sin(\phi_N-\phi_H)]\dot{\theta}_H^2 + [m_H L_N L_H\,\sin\theta_N\sin\theta_H\sin(\phi_N-\phi_H)]\dot{\phi}_H^2 \\
& + (\beta_{\phi N} + \beta_{\phi H})\phi_N - \beta_{\phi H}\phi_H + (m_N l_N + m_H L_N)\,(-\ddot{x}\,\sin\theta_N\sin\phi_N + \ddot{y}\,\sin\theta_N\cos\phi_N) = 0
\end{aligned}
$$

$$
\begin{aligned}
\theta_H :\ & \{m_H L_N L_H\,[\cos\theta_N\cos\theta_H\cos(\phi_N-\phi_H) + \sin\theta_N\sin\theta_H]\}\ddot{\theta}_N + [m_H L_N L_H\,\sin\theta_N\cos\theta_H\sin(\phi_N-\phi_H)]\ddot{\phi}_N \\
& + (m_H L_H^2 + I_{yy}^P)\ddot{\theta}_H - I_{yz}^P\ddot{\phi}_H - [2\, m_H L_N L_H\,\sin\theta_N\cos\theta_H\cos(\phi_N-\phi_H)]\dot{\phi}_N\dot{\phi}_H \\
& + \{m_H L_N L_H\,[-\sin\theta_N\cos\theta_H\cos(\phi_N-\phi_H) + \cos\theta_N\sin\theta_H]\}\dot{\theta}_N^2 + [m_H L_N L_H\,\sin\theta_N\cos\theta_H\cos(\phi_N-\phi_H)]\dot{\phi}_N^2 \\
& - [m_H L_H^2\,\cos\theta_H\sin\theta_H]\dot{\phi}_H^2 - \beta_{\theta H}\theta_N + \beta_{\theta H}\theta_H \\
& + m_H L_H\,[\,\ddot{x}\,\cos\theta_H\cos\phi_H + \ddot{y}\,\cos\theta_H\sin\phi_H - (\ddot{z} + g)\sin\theta_H] = 0
\end{aligned}
$$

$$
\begin{aligned}
\phi_H :\ & [m_H L_N L_H\,\cos\theta_N\sin\theta_H\sin(\phi_N-\phi_H)]\ddot{\theta}_N + [m_H L_N L_H\,\sin\theta_N\sin\theta_H\cos(\phi_N-\phi_H)]\ddot{\phi}_N \\
& - I_{yz}^P\ddot{\theta}_H - (m_H L_H^2\sin^2\theta_H + I_{zz}^P)\ddot{\phi}_H - [m_H L_N L_H\,\sin\theta_N\sin\theta_H\sin(\phi_N-\phi_H)]\dot{\theta}_N^2 \\
& - [m_H L_N L_H\,\sin\theta_N\sin\theta_H\sin(\phi_N-\phi_H)]\dot{\phi}_N^2 + [2\, m_H L_N L_H\,\cos\theta_N\sin\theta_H\cos(\phi_N-\phi_H)]\dot{\theta}_N\dot{\phi}_N \\
& + [2\, m_H L_N L_H\,\sin\theta_N\cos\theta_H\cos(\phi_N-\phi_H)]\dot{\theta}_H\dot{\phi}_N - [2\, m_H L_H^2\,\sin\theta_H\cos\theta_H]\dot{\theta}_H\dot{\phi}_H \\
& - \beta_{\phi H}\phi_N + \beta_{\phi H}\phi_H + m_H L_H\,(-\ddot{x}\,\cos\theta_H\cos\phi_H + \ddot{y}\,\cos\theta_H\sin\phi_H) = 0
\end{aligned}
$$

process was used to approximate possible solutions and to aid in the understanding of the model parameters.

Linearization of the equation set was accomplished in two ways. The first assumption made was that the angles of displacement, i.e. the solutions to the system, would deviate only slightly from their equilibrium positions. The equilibrium positions chosen were the initial positions for the particular head-neck-helmet configuration used during a data run. This approximation necessitated the substitution of an expression which defined a large angle of displacement as the sum of its initial angle and the small deviation. For example,

$$\Theta_H = \theta_H + \theta_{HO}$$

where Θ_H is the large angle of displacement,

θ_{HO} is the initial angle at equilibrium,

θ_H is the angular displacement from the equilibrium position.

This substitution was made for each of the four generalized coordinates.

The second approximation involved neglecting the second and higher order terms in the equation set. Since the angles of displacement were assumed to be small and the magnitude of the excitation was defined as of small amplitude, the contribution of these terms would be negligible; thus, this approximation was considered a reasonable assumption.

These assumptions reduce the generalized equation set to the form

$$[\mathbf{M}]\ \{\ddot{q}_i\} + [\mathbf{K}]\ \{q_i\} + \mathbf{mL}\ \{\mathbf{A}\} = \{0\}$$

The equations in this linearized set are presented in Table 4. The full procedure is provided in Appendix B.

TABLE 4
LINEARIZED EQUATIONS OF MOTION

$$\theta_N : \quad (m_N l_N^2 + m_H L_N^2 + I_{yy}^{O})\ddot{\theta}_N - I_{yz}^{O}\ddot{\phi}_N + \{m_H L_N L_H \,[\cos\theta_{NO}\cos\theta_{HO}\cos(\phi_{NO}-\phi_{HO}) + \sin\theta_{NO}\sin\theta_{HO}]\}\ddot{\theta}_H$$

$$+ [m_H L_N L_H \,\cos\theta_{NO}\sin\theta_{HO}\sin(\phi_{NO}-\phi_{HO})]\ddot{\phi}_H + (\beta_{\theta N} + \beta_{\theta H})(\theta_N + \theta_{NO}) - \beta_{\theta H}(\theta_H + \theta_{HO})$$

$$+ (m_N l_N + m_H L_N)\,[\ddot{x}\,\cos\theta_{NO}\cos\phi_{NO} + \ddot{y}\,\cos\theta_{NO}\sin\phi_{NO} - (\ddot{z} + g)(\sin\theta_{NO} + \theta_N\cos\theta_{NO}] = 0$$

$$\phi_N : \quad - I_{yz}^{O}\ddot{\theta}_N + [(m_N l_N^2 + m_H L_N^2)\sin^2\theta_{NO} + I_{zz}^{O}]\ddot{\phi}_N + [m_H L_N L_H \,\sin\theta_{NO}\cos\theta_{HO}\sin(\phi_{NO}-\phi_{HO})]\ddot{\theta}_H$$

$$+ [m_H L_N L_H \,\sin\theta_{NO}\sin\theta_{HO}\cos(\phi_{NO}-\phi_{HO})]\ddot{\phi}_H + (\beta_{\phi N} + \beta_{\phi H})(\phi_N + \phi_{NO}) - \beta_{\phi H}(\phi_H + \phi_{HO})$$

$$+ (m_N l_N + m_H L_N)\,(-\ddot{x}\,\sin\theta_{NO}\sin\phi_{NO} + \ddot{y}\,\sin\theta_{NO}\cos\phi_{NO}) = 0$$

$$\theta_H : \quad \{m_H L_N L_H \,[\cos\theta_{NO}\cos\theta_{HO}\cos(\phi_{NO}-\phi_{HO}) + \sin\theta_{NO}\sin\theta_{HO}]\}\ddot{\theta}_N + [m_H L_N L_H \,\sin\theta_{NO}\cos\theta_{HO}\sin(\phi_{NO}-\phi_{HO})]\ddot{\phi}_N$$

$$+ (m_H L_H^2 + I_{yy}^{P})\ddot{\theta}_H - I_{yz}^{P}\ddot{\phi}_H - \beta_{\theta H}(\theta_N + \theta_{NO}) + \beta_{\theta H}(\theta_H + \theta_{HO})$$

$$+ m_H L_H \,[\ddot{x}\,\cos\theta_{HO}\cos\phi_{HO} + \ddot{y}\,\cos\theta_{HO}\sin\phi_{HO} - (\ddot{z} + g)(\sin\theta_{HO} + \theta_H\cos\theta_{HO})] = 0$$

$$\phi_H : \quad [m_H L_N L_H \,\cos\theta_{NO}\sin\theta_{HO}\sin(\phi_{NO}-\phi_{HO})]\ddot{\theta}_N + [m_H L_N L_H \,\sin\theta_{NO}\sin\theta_{HO}\cos(\phi_{NO}-\phi_{HO})]\ddot{\phi}_N$$

$$- I_{yz}^{P}\ddot{\theta}_H - (m_H L_H^2\sin^2\theta_{HO} + I_{zz}^{P})\ddot{\phi}_H - \beta_{\phi H}(\phi_N + \phi_{NO}) + \beta_{\phi H}(\phi_H + \phi_{HO})$$

$$+ m_H L_H \,(-\ddot{x}\,\cos\theta_{HO}\cos\phi_{HO} + \ddot{y}\,\cos\theta_{HO}\sin\phi_{HO}) = 0$$

III. COMPUTER IMPLEMENTATION

To test the validity of the linear equation set, a comparison between the experimental human data and the mathematical model equations was needed. To perform this comparison, a frequency domain solution to the linear equations of motion was required. Because of the complexity of the linear equation set (due to its time dependent coefficients), a computer program would be needed to solve the equations of motion for the four generalized coordinates (θ_N, θ_H, ϕ_N, ϕ_H). To simplify the computer program implementation, the remainder of this preliminary study was concerned with the solution to one equation of the set -- the equation derived from the θ_H generalized coordinate -- to test its solution against the experimental human data. The decision to investigate only one equation greatly reduced the complexity of the solution process, while maximizing efforts to perform data comparisons.

To solve the θ_H equation of motion, several tasks were accomplished; these included specifying the forcing function, designing the frequency solution algorithm, considering the time domain amplitude of θ_H, and selecting the head-helmet physical parameters.

Forcing Function Specification

To simplify the equation system further, the form of vibration excitation, i.e. the forcing function, was specified. A sinusoidal force was chosen, which reduced the complexity of the θ_H equation and aided in the solution for θ_H.

The θ_H equation in its linear form appeared as,

$$(m_H L_H^2 + I_{YY}^P)\,\ddot{\theta}_H + \beta_{\theta H}\,(\theta_{HO} + \theta_H)$$
$$+ m_H L_H\,[\ddot{x}\cos\theta_{HO} - (\ddot{z} + g)\,(\sin\theta_{HO} + \theta_H\cos\theta_{HO})] = 0$$

By specifying a sinusoidal excitation of

$$x = A_x \sin\Omega t \quad , \qquad z = A_z \sin\Omega t$$

and a response of

$$\theta_H = T_H \sin\Omega t$$

and applying the appropriate derivatives, the θ_H equation was reduced to

$$[-(m_H L_H^2 + I_{YY}^P)\,\Omega^2 + \beta_{\theta H}]\,T_H \sin\Omega t + \beta_{\theta H}\theta_{HO}$$
$$+ m_H L_H\,[-\Omega^2 A_x \sin\Omega t\,\cos\theta_{HO}$$
$$-(-\Omega^2 A_z \sin\Omega t + g)\,(\sin\theta_{HO} + T_H \sin\Omega t\,\cos\theta_{HO})] = 0$$

In addition, the input excitation was limited to the z direction for simplicity of comparison. This further reduced the equation to

$$T_H \left[-(m_H L_H^2+I_{yy}^P)\,\Omega^2 - m_H L_H(g - \Omega^2 A_z \sin\Omega t)\cos\theta_{HO} + \beta_{\theta H}\right]$$

$$- m_H L_H \sin\theta_{HO}\left[\frac{g}{\sin\Omega t} - \Omega^2 A_z \sin\Omega t\right] + \frac{\beta_{\theta H}\,\theta_{HO}}{\sin\Omega t} = 0$$

For the equation T_H, the solution took the form

$$T_H = \frac{\left[\dfrac{m_H L_H \sin\theta_{HO}\, g - \beta_{\theta H}\,\theta_{HO}}{\sin\Omega t}\right] - \Omega^2 A_z\, m_H L_H \sin\theta_{HO}}{-(m_H L_H^2+I_{yy}^P)\,\Omega^2 - m_H L_H(g - \Omega^2 A_z \sin\Omega t)\cos\theta_{HO} + \beta_{\theta H}}$$

Finally, it followed from static equilibrium and the definition of θ_{HO} that

$$\beta_{\theta H}\,\theta_{HO} - m_H\, L_H\, g \sin\theta_{HO} = 0$$

This final observation reduced the T_H equation to

$$T_H = \frac{m_H\, L_H\, A_z \sin\theta_{HO}}{m_H L_H^2+I_{yy}^P - m_H L_H\, A_z \sin\Omega t + \left[\dfrac{m_H L_H g\cos\theta_{HO} - \beta_{\theta H}}{\Omega^2}\right]}$$

This was the form of the equation used in the solution algorithm.

Frequency Solution Algorithm

The comparison of numerical and experimental data required that the computational solution to the θ_H equation be presented in the frequency domain. This requirement meant that the solution should express the θ_H response due to a change in the frequency or presence of the forcing function. As derived, the θ_H equation was a time domain, or time dependent, solution. Direct mathematical transformation of the equation from the time to the frequency domain by Laplace or Fourier transforms was one possible method; for ease of implementation, a numerical solution was devised which produced time ordered data, which was then converted to the frequency domain.

The flow chart in Figure 2 indicates the steps to the numerical solution process. The equation was mathematically solved for T_H, and placed within the time solution block. The program began sinusoidal excitation of the system at 1.0 Hz and collected the values of T_H for each 0.02 second time step over a period of 2.0 seconds. The program then made incremental steps of 0.5 Hz, collecting the data over the same 2.0 second period, and adding the responses to the time data collection. In this way, the system was sinusoidally excited at each of the incremental steps up to 25 Hz. The end result was a collection of time dependent data points which expressed the summed responses over the range of excitation from 1 to 25 Hz. This

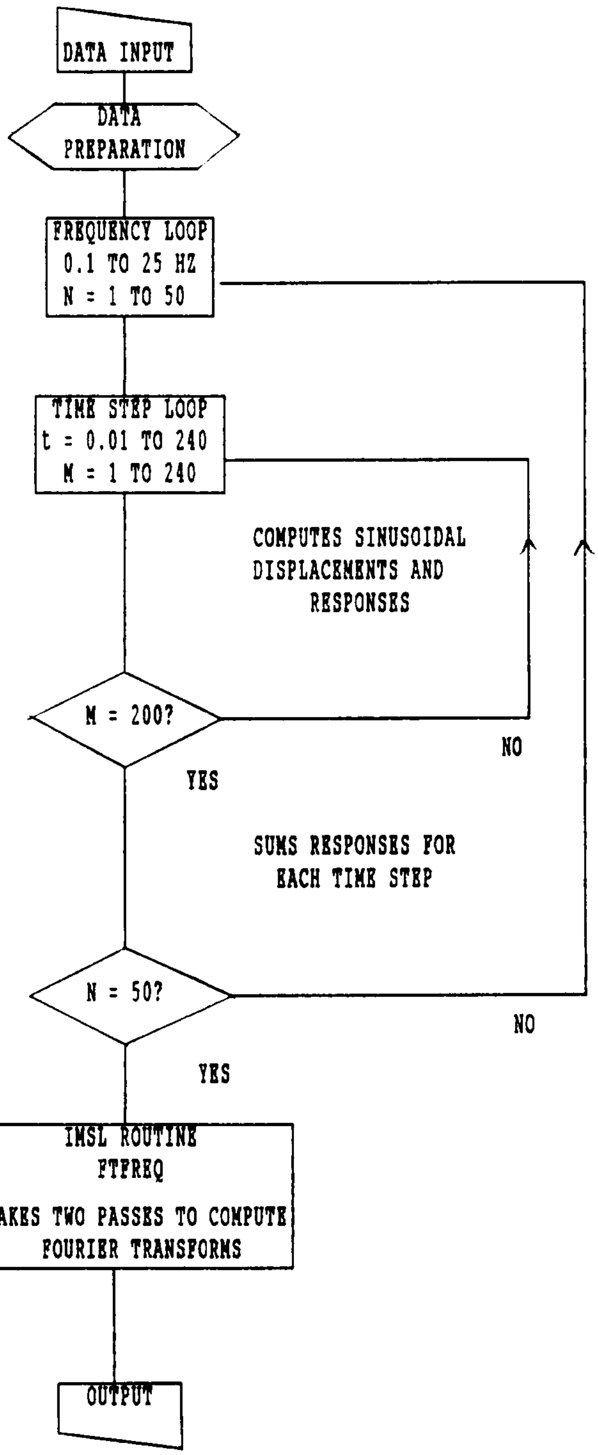

Figure 2. Flowchart for ONEEQ.FOR.

collection of time data was then processed using the IMSL subroutine FTFREQ (IMSL, 1984), a Fourier analysis program, which transformed the time data into the required frequency information.

The program which performed these calculations was named ONEEQ.FOR. This program was written in FORTRAN and is listed in Appendix C. The data input consisted of physical parameters of the head-helmet system, such as head mass and CG, helmet mass and CG, and the spring constant $\beta_{\theta H}$. The output data was the frequency response between the sinusoidal excitation force and corresponding θ_H deflection. Output parameters included the real and imaginary coefficients, the phase angle, and the coherence of the response (components of the frequency response).

Small Amplitude Considerations

Upon development of the computer algorithm, one aspect of the model was cautiously noted. The formulation of the equation and the design of the algorithm did not take into account the inclusion of a damping, or energy absorption, factor. From the general equation, it was noted that any solution at a resonant frequency would produce an amplitude of infinite proportions. Solutions near resonant frequencies would then violate the small angle assumption made in the development of the equation system.

This particular problem was dealt with in the production of the time domain data. As the spring stiffness $\beta_{\theta H}$ was varied for data comparisons, the time data was monitored to check for large angles of deflection. If such angles were detected, then the spring constant was adjusted slightly to move the solution out of the large angle range. With this procedure, the model's solution to the θ_H equation would not specify the actual natural frequency, but the solution would be very near it.

Physical Parameter Selection

Several physical parameters were required for the solution to the θ_H equation:

(1) mass of the neck,
(2) mass and inertial properties of the head,
(3) mass and inertial properties of the helmet,
(4) positions of the neck CG and the head-helmet CG, and
(5) the stiffness for the $\beta_{\theta H}$ spring.

Because of the variations in the head and neck sizes in the experimental population of military subjects, a standard size for the head and neck was used for the computer solution. These measurements, which appear in Table 5 were taken from the Army standard for the 50th percentile Army aviator (Department of Defense, 1985). Use

TABLE 5

BODY PARAMETERS FOR 50TH PERCENTILE AVIATOR

Body Parameter	Mass (Kg)	Location (cm) x	y	z	Moments of Inertia (Kg·cm²) I_{xx}	I_{yy}	I_{zz}
Neck CG	1.06	1.1	0.0	5.0	17	21	26
Head CG	4.24	2.4	0.0	15.2	198	226	147
A-OC Pivot	--	2.0	0.0	11.0	--	--	--

Note: CG and pivot locations are relative to the C7-T1 junction. Head moments of inertia are measured at the Head CG.

of these measurements was assumed to be acceptable for later comparison with the experimental data.

The helmet mass and inertia products were selected from conditions used in the experimental procedure. The helmet parameters approximated several types of current military designs, listed in Table 6. These parameters were combined with the head parameters to form a single head-helmet unit of mass and inertial properties. A CG for the combined unit was calculated and used in the model. Five different caseloads were designed for comparison with the experimental data, also shown in Table 6.

Values for the β_{OH} spring were selected in accordance with experimental results. This parameter was varied in order to produce amplitudes which matched the experimental findings. The change in the spring constant

TABLE 6

HELMET PROPERTIES FOR VARIABLE CG HELMET

Helmet Configuration	Helmet Description	CG (cm) x	y	z	Helmet Moment of Inertia (Kg·cm²) I_{xx}	I_{yy}	I_{zz}
Center	None	0	0	0	348	52	296
High	SPH-4	0	0	2	310	14	296
Front	NVG	2	0	0	348	64	309
Side	IHADSS	0	2	0	338	55	286
2.95 Kg Helmet	None	0	0	0	616	33	583

Note: Helmet configuration describes the CG location. Helmet description is used for comparison to similar Army aviator helmets: SPH-4 is standard issue; NVG is an SPH-4 with night vision goggles attached; IHADSS is a helmet with a heads-up display. Each helmet had a mass of 2.04 Kg (with the exception of the 2.95 Kg helmet). CG is relative to the intersection of a line through the ear canals with the mid-sagittal plane of the head. Helmet moments of inertias are measured relative to this point.

indicated changes in the system due to loading or change in CG. By examining the trends in these variations, an explanation was derived concerning muscle compensation and mechanism.

IV. RESULTS

Data from the computational model were evaluated for the five cases described in Section III. These results were compared to the experimental human data from the Maday and Butler (1985) investigation, the comparisons being limited to evaluations of data from three experimental subjects. The experimental data was evaluated using a Nicolet 660 Signal Analyzer. The computational data was calculated on a DEC VAX 11/780. The data comparisons concerned general trends in frequency responses, apparent displacement, and spring constant changes.

General Observations

The model frequency data were fit to the experimental frequency data using the imaginary domain of each response. This comparison was used since the experimental frequency data did not exhibit as readily recognizable resonances in the graph of the magnitude function as in that of the imaginary function.

The computational solution algorithm produced a single resonant peak near 5 Hz for each of the five cases. This corresponded to the general response noted in the experimental data at the same frequency. Spot comparisons of experimental accelerometer data identified this motion as a characteristic flexion-extension, or "head bobbing", motion about a centralized position. Although the computational solution often showed several harmonic peaks, the resonance near 5 Hz is clearly dominant.

Static equilibrium values for the stiffness of the $\beta_{\Theta H}$ spring for each case were found to be insufficient to produce motion greater than that of the z excitation alone. Values between 100 and 130 N-cm/rad produced some greater responses, but the motion continued to follow the motion of the z excitation. This condition was identified by continuous positive angles of deflection away from the equilibrium point, indicating flexion of the head from the rest position.

Spring values between 130 N-cm/rad and 210 N-cm/rad produced deflections which indicated movement above and below the initial equilibrium point. The time values showed both positive and negative deflections during the z excitation. Stiffness constants in this range were used to evaluate the model performance concerning mass and CG effects. The exact values used are presented in Table 7, along with the values calculated for static equilibrium for each case.

TABLE 7

SPRING CONSTANTS UTILIZED FOR $\beta_{\theta H}$ IN NUMERICAL ANALYSIS OF MODEL FREQUENCY CHARACTERISTICS

TREATMENT	CALCULATED STATIC VALUES N•cm/rad	REQUIRED DYNAMIC VALUES N•cm/rad	TYPE OF HELMET LOADING
MASS EFFECTS	33.0	150.0	CENTER 2.04 kg
	54.2	150.0	CENTER 2.95 kg
CENTER OF GRAVITY EFFECTS	33.0	156.0	CENTER 2.04 kg
	58.4	168.0	FRONT 2.04 kg
	74.0	159.0	TOP 2.04 kg
	49.3	150.5	SIDE 2.04 kg

Finally, spring values above 210 N-cm/rad showed continuous negative deflections, meaning that the motion was above the initial equilibrium point. These values of deflection over time indicated the head being extended from its rest position.

Effects of Changing Mass

Experimental data from Subject 1 were used for the comparison pictured in Figure 3. A spring constant of 150 N-cm/rad proved to be a satisfactory value to simulate the experimental response of the center-weighted 2.04 kg helmet. Figure 3 shows the upward spike produced by the model near 5 Hz. This corresponds to the peak in the experimental data at approximately 4 Hz. Although, these peaks are not at exactly the same frequency, they do exhibit similar trends.

For the 2.95 kg center-weighted helmet, the spring constant was held at 150 N-cm/rad to see the effects of the increased mass. Figure 3 shows the same peaks near 4 and 5 Hz as exhibited earlier, but the magnitude and direction of these peaks are different. Notice that the experimental data curve is smoother than for the 2.04 Kg helmet.

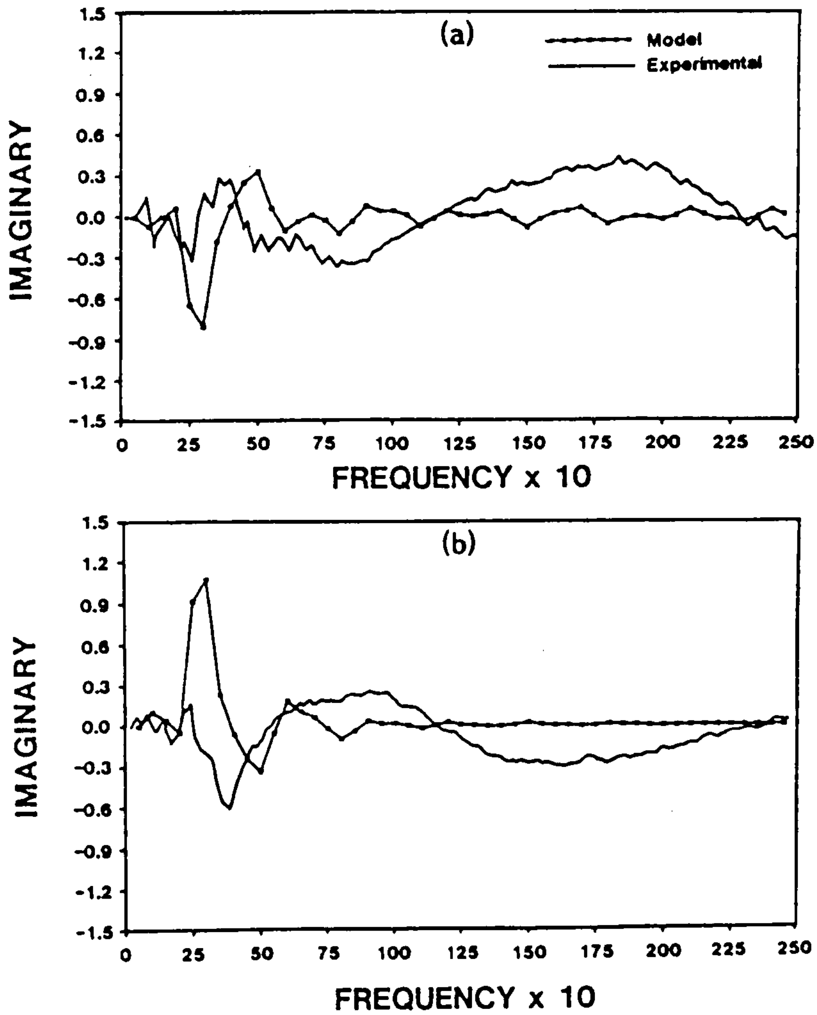

Figure 3. Effects of Increased Mass on Head-Helmet Frequency Characteristics. Plots show Frequency x 10 vs. Imaginary coefficients of transfer function (Z axis response) for (a) 2.04 kg helmet and (b) 2.95 kg helmet, during Z axis excitation, for both experimental and model data.

Effects of Changing Center-of-Gravity

For this comparison, a change in the spring constant accompanied the change in CG. The change was made to match the experimental data for each case. In this way, the change in spring stiffness would match the change in muscle tension due to changing CG and inertial properties. Experimental data from Subject 3 were used in the comparison pictured in Figure 4.

The center-weighted helmet was again chosen as a starting point with its spring constant set at 156 N-cm/rad. Figure 4a shows the resonance indicated near 5 Hz. The model data fit closely with the experimental data.

In Figure 4b, the front-weighted helmet data shows some instability. The spring constant was raised to 168 N-cm/rad to match the experimental data. The solution was very unstable in this range, making the spring constant hard to select.

The spring constant was set at 159 N-cm/rad for the top-weighted helmet. The computer solution closely simulated the experimental curve, as shown in Figure 4c. This solution proved stable and was easily computed.

Finally, the side-weighted helmet was found to be very unstable. Although its spring constant was reduced to 150 N-cm/rad, the value was hard to choose due to the small

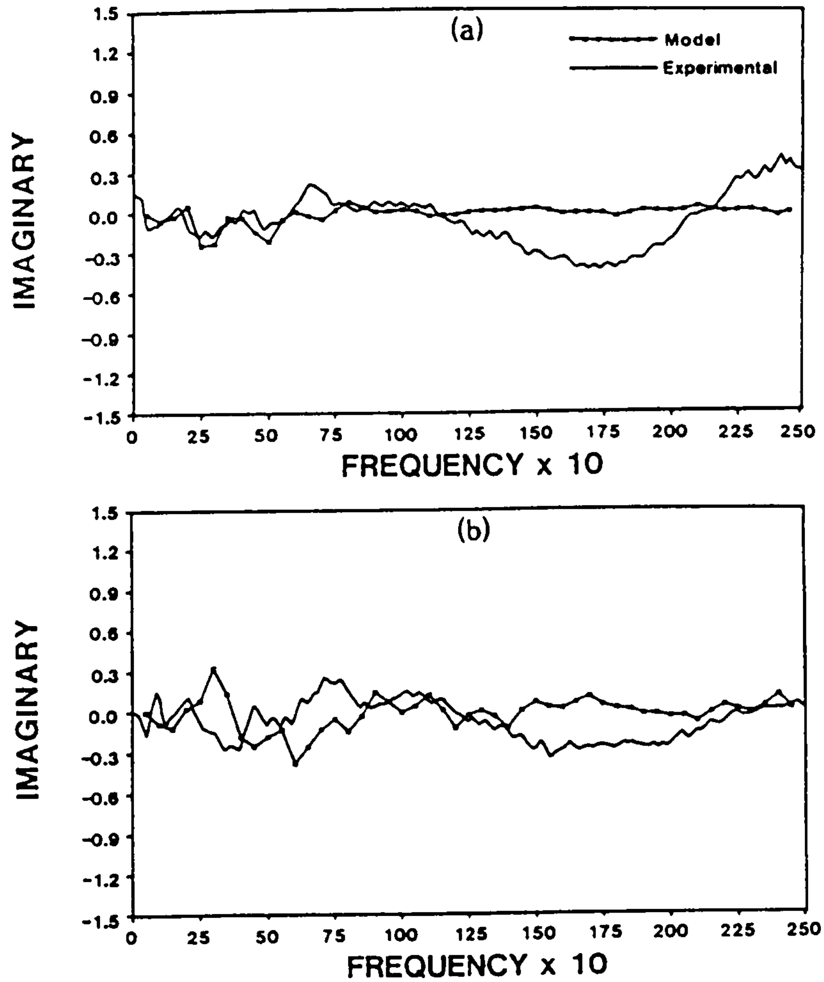

Figure 4. Effects of Changing Center-of-Gravity on Head-Helmet Frequency Characteristics. Plots show Frequency x 10 vs. Imaginary coefficients of transfer function (Z axis response) for (a) center-loaded, (b) front-loaded, (c) top-loaded, and (d) side-loaded helmets during Z axis excitation, for both experimental and model data.

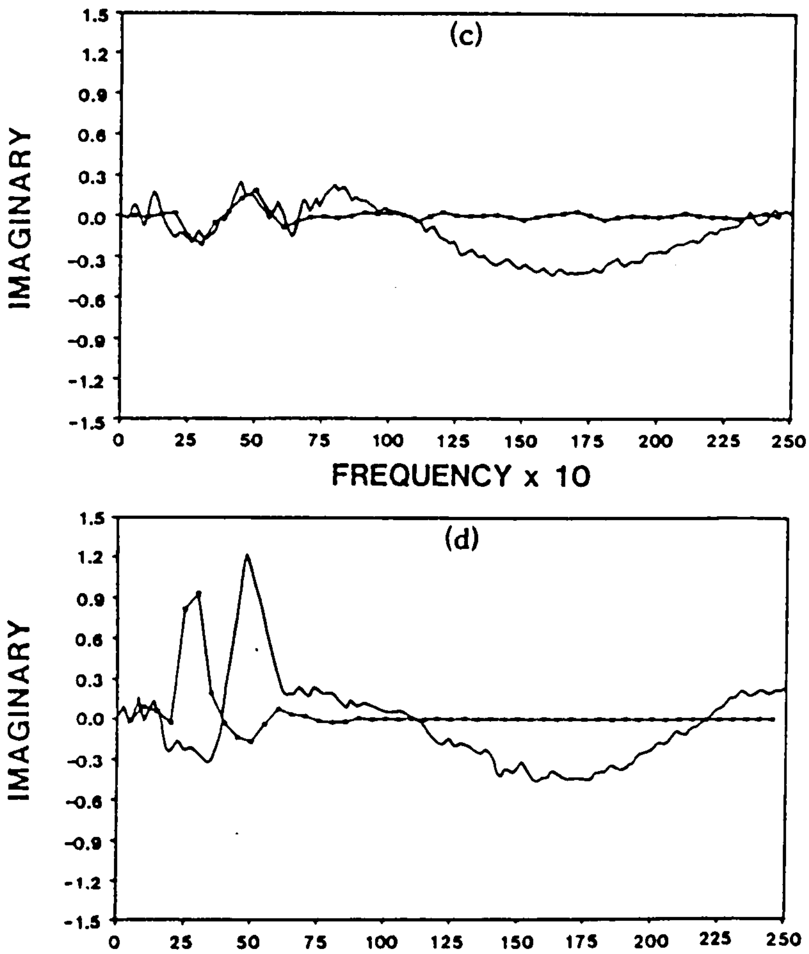

Figure 4 - continued.

range of compatibility the solution exhibited. Figure 4d shows the comparison between the experimental and model data.

V. CONCLUSIONS

An analysis of the results revealed insights not only into the effects of changes in basic helmet design, but also established some explanations concerning muscle recruitment mechanisms of the head-neck system. Further observations provided explanations of model performance and recommendations for improvements to model formulation and solution.

Discussion of Results

There were several interesting trends which appeared in the data that were not expected. These trends lead to some insights into types of compensation mechanisms exhibited by the body (particularly, the muscles of the head and neck) for changes in loading conditions.

In the first investigation concerning mass changes, only the mass of the helmet was changed, while the CG of the helmet was maintained. In the experimental (physical) data, this change in mass corresponded to a change in direction and amplitude for several resonant peaks. The peak near 5 Hz, which represented the "head-bobbing" motion, showed a change from 0.3 to -0.6, denoting a change in amplitude as well as direction. Corresponding changes were seen in the model, although the change in amplitude was not as great (from 0.3 to -0.3).

These results demonstrated the model's ability to represent a change in motion due to changes in mass, although changes in amplitude might not be directly proportional to that exhibited by the physical data.

Another aspect considered was the change in resonant frequency due to the change in mass. Notice that a slight shift was seen in the resonant frequency of the model as the mass is increased, while the physical data remained essentially the same. Remember that for this investigation, the spring constant of the model was maintained at 150 N-cm/rad for both cases; thus, a change in resonant frequency might be expected as the mass was changed. Consider the basic equation for calculating natural frequency:

$$f_N = \frac{1}{2\pi} \left[\frac{k}{m} \right]^{\frac{1}{2}}$$

A decrease in frequency, not an increase as seen in the data, would be expected as mass increases. In addition, no such change in frequency was seen in the physical data at all.

One explanation for the characteristics exhibited by the model was that the change in mass of the helmet has altered the combined head-helmet CG enough to cause the frequency increase. The mass change altered the CG, thus reducing the length of the rod (L_H) and increasing the initial angle (θ_{HO}). By keeping the spring constant, these changes in length and initial rotation were enough to cause a frequency increase.

As noted, the physical data did not exhibit this change in frequency. One explanation was the way the body reacted to the increased load. In the body's attempt to maintain equilibrium or initial position, additional muscle groups were called upon to share the new load. This reaction where the number of active muscle fibers depends on load was known as recruitment. By increasing the number of muscle fibers used, the effective stiffness of the system was increased. The frequency equation noted earlier would show a increase in the natural frequency for such a change. Therefore, since both the mass of the head-helmet and the effective stiffness were changed simultaneously, the natural frequency at 5 Hz was maintained. Again, the model did not exhibit this constant frequency due to keeping the stiffness of the spring constant.

These findings showed that an increase in mass caused a change in the motion of the head-helmet system while also maintaining a constant resonant frequency. The physical data indicated that an increase in amplitude also accompanied the increase in mass, while the model did not show this increase. This increase in the physical data might indicate that the large mass helmet (2.94 kg) could cause greater problems for subjects performing tasks (such as target tracking) than the small mass helmet (2.04 kg).

The second investigation concerning changes in CG also provided interesting results. The overall effects appeared to concern the stability of the head-neck-helmet system and the maintenance of a constant resonant frequency. Changing the spring constant aided the model in mimicking the body's reactions, while also providing insights to explain the nature of these reactions.

One noticeable difference between load cases was the stability of the model solution. For the center and top loaded helmets, the model solution was more stable over a wide range of values chosen to fit the physical data. Often, values could vary as much as 2 N-cm/rad above or below the selected value before significant changes were seen in the solution. On the other hand, the front and side loading cases were much more sensitive to such changes. Changes as small as 0.2 N-cm/rad caused radical changes in the solution, such as infinite displacements or sudden drops to no displacement.

These changes in the stability of the model solution seemed to correspond to the reaction of the body to these changes, as exhibited by the physical data. The center and top loading cases exhibited fairly smooth reactions to their loading situations, showing small but stable displacements over the frequency range from 0-10 Hz and a distinct separation between modes of vibration. Conversely, the front- and side-loaded helmets produced reactions in this same range which were large and appeared to contain many coupled modes of vibration.

These stability and reactivity changes also seemed to indicate that the front- and side-loaded helmets were not as suitable for use in these types of vibration situations as the center- and top-loaded helmets. The bodily reactions to these helmets might cause the human subject to be more susceptible to environmental vibrations which could reduce the subject's ability to perform adequately in an operational situation.

Another factor which might have heightened these trends was the body's ability to maintain a particular resonant frequency despite changes in CG. Each of the four loading cases exhibited the resonance associated with "head bobbing" located near 5 Hz. The data in both the model and physical examples showed larger displacements for the front- and side-loaded helmets as compared to the other cases. If an operational situation should involve an environment with a 5 Hz excitation, a person wearing a front- or side-loaded helmet would obviously have more difficulty performing duties (such as tracking tasks) than would someone wearing a top- or center-loaded helmet.

The effect of maintaining a particular frequency again appeared to be explained by the mechanism of recruitment. The data in the results section concerning the changes in the model's spring constant supported this conclusion. As loading was changed from the center to the front, the required spring constant was increased from 156 to 168 N-cm/rad. As the loading was changed to the top, the spring constant was decreased to 159 N-cm/rad, only slightly larger than the center loaded case. These cases exhibited the increase in the spring stiffness over the center loaded case, which would correspond to the increased muscle recruitment for these loads.

The constant for the side load was decreased even further to 150 N-cm/rad. Although this would seem inconsistent with the other results, the explanation was simple. The side loading would physically require the recruitment of muscles which were not represented by the $\beta_{\theta H}$ spring; thus, the load was reduced on the $\beta_{\theta H}$ spring while the "unknown spring" began to share the load. In this case, the model was unable to accurately reproduce the entire mechanism, but did an adequate job of revealing the general trends.

In summary, it appeared that the large mass helmet, the front-loaded helmet, and the side-loaded helmet were undesirable configurations for subjects in environments with excitations near 5 Hz. These helmets, because of their effects on the human head-neck system, might cause a decrease in effective performance of some duties, particularly in the realm of target tracking.

Observations and Recommendations

Although the model performed adequately for this analysis using one degree of freedom, there were several observations and recommendations that could be made which would enhance the performance of the model. These changes would not only improve the validity of the model, but they would also provide clearer answers to questions concerning the vibration characteristics of the human head-neck system. These observations and proposed changes fell into four categories:

1. Change of coordinate system
2. Change in spring implementation
3. Addition of damping
4. Improvement of solution algorithm

The spherical coordinate system that was chosen for the four degree of freedom system was adequate to explain the rotations proposed about the y and the z axes. Physically, however, there was a lateral rotation of the head and neck which the present form of the model could not represent. A rotation about the x axis at both pivots could be added to the analysis, therefore increasing the number of degrees of freedom to six.

Another alternative was to change the type of coordinate system used. A system described using Euler angles may be more suitable, since a majority of the motion described exhibit near-gyroscopic motion. Using such a system might allow a complete description of the true physical motion, while using only five degrees of freedom.

As was noted in Section IV, the values expressed as "static spring constants" for the loading cases were less than that which was required to assure motion of the system. The dynamic values were often two to four times that of the static values. This result could be easily explained and possible changes to the system proposed. When the model was "at rest", the spring value was calculated from the derived static condition. The rotational spring could be given this value to simulate this static state, if desired. The situation corresponded to the use of muscle recruitment of fibers within extensor muscles such as the rectus capitis posterior major and minor, pulling the head-neck assemblage up into a resting position (a muscle is like a cable and can only act in tension). The flexor muscles for the head, such as the rectus capitis anterior, would be relaxed and not contributing to the force needed to produce static equilibrium. For this situation, the rotational spring could effectively reproduce the static force caused by this one-directional pull when using the calculated static value. This description was rather simplistic; actually, the static value represented the difference in stiffness between the extensor and flexor muscles, with the extensors exerting the greater force to maintain equilibrium.

When excitation was added to the physical system, a dynamic change was produced in the system which required both sets of muscles to interact simultaneously. This type of interaction produced a resultant force at the pivot which was greater than the required static force. In similar studies involving joints, Brewster, et.al. (Walker, 1977) measured these forces at 1.8 to 4.36 times that experienced at rest. In order for the model to accurately reproduce this change, the rotational spring constants must fall in the same range.

With this fact in mind, two courses of action could be attempted. First, additional computations could be performed for each case to determine the resultant force appearing in the analysis; then the value of the rotational spring could be adjusted to produce such a force. Second, a system of linear springs could be used to simulate the actions of the individual extensor and flexor muscle groups. Either solution might have slight drawbacks, but such changes would improve the model's ability to reproduce muscle function.

Possibly a major drawback to the model was the absence of a damping factor. The inclusion of damping would increase the stability of the solution by limiting the amplitude of the response at resonance. This factor could be especially useful in terms of maintaining the small angle approximation and increasing the validity of the theoretical development. A damping coefficient around 19% should be adequate to simulate normal joint function (Wasserman, 1983).

Finally, a more accurate algorithm would improve the solution process. Although the algorithm utilized was adequate, an improved solution would reduce errors, such as truncation and round-off error, by more efficient means of calculation. A first step may be analytically solving the equation set using Laplace or Fourier transforms. Attempts should start with the one degree of freedom system in this analysis and continue with validation runs to test the solution before adding additional degrees of freedom.

Other recommendations could be made to further improve the system, but these basic changes should be considered first before attempting more complicated processes. The solution to a model using some or all of these suggestions would undoubtedly answer questions left unanswered here, but would also produce additional questions in turn.

LIST OF REFERENCES

LIST OF REFERENCES

Ewing, C. L. and Thomas, D. J. "Human head and neck response impact acceleration." Naval Aerospace Medical Research Detachment, New Orleans, Monograph 21, 1972.

The 50th Percentile Standard Military Aviator for Male Human Analogue. Draft Military Standard. Department of Defense, 1985.

Frisch, G. D. and Cooper, C. "Mathematical modeling of the head and neck response to -Gx impact acceleration (minimum articulation requirements)." Aviation, Space, and Environmental Medicine. 49(1):196-204, 1978.

Gray, Henry. Anatomy of the Human Body, 28th edition, Charles M. Goss, editor. Lea and Feiber, 1966.

Greenwood, D. T. Principles of Dynamics. Prentice-Hall, Inc., 1965.

International Mathematical and Statistical Library. "IMSL Routine Name - FTFREQ." IMSL Documentation, 1984.

Jex, H. R. and Magdaleno, R. E. "Biomechanical models for vibration feedthrough to hands and head for a semisupine pilot." Aviation, Space, and Environmental Medicine. 49(1):304-316, 1978.

Maday, R. E. and Butler, B. P. Unpublished data relating to Vibration Research. US Army Aeromedical Research Laboratory, 1985.

Schneider, L. W., and Bowman, B. M. "Prediction of head/neck dynamic response of selected military subjects to -Gx acceleration." Aviation, Space, and Environmental Medicine. 49(1):221-223, 1978.

Smith, D. E. and Anderson, W. R. "Predictive model of dynamic response of the human head/neck system to -Gx impact acceleration." Aviation, Space, and Environmental Medicine. 49(1): 224-233, 1978.

Viviani, P. and Berthoz, A. "Dynamics of the head-neck system in response to small perturbations: analysis and modeling in the frequency domain." Biological Cybernetics. 19:19-37, 1975.

Walker, Peter S. Human Joints and Their Artificial Replacements. Charles C. Thomas Publishers, 1977.

Wasserman, J. F. Unpublished data concerning vibration analysis of variable weight/CG helmet. University of Tennessee, Knoxville, 1984.

Wasserman, J. F., Weigel, J. P., and Pickard, C. A. "Vibration Evaluation of Degenerative Joint Disease." Proceedings Of 36th ACEMB Conference, p. 8, 1983.

APPENDIXES

APPENDIX A

DEVELOPMENT OF NONLINEAR EQUATION SYSTEM

SYSTEM REPRESENTATION

The system to be modeled was that of the human head and neck subjected to vibratory motion in three directions. The system was made up of point masses located on massless rods which are constrained by rotational springs. The head representation included the addition of a helmet mass and its inertial properties. Spherical coordinates were selected as the generalized coordinates for the Lagrange formulation, with the length of the rods remaining constant. This allowed the system to be described in four degrees of freedom using the generalized coordinates θ_N, ϕ_N, θ_H, ϕ_H. (Refer to Section II, Figure 1, p.10 for graphic representation.)

GENERALIZED COORDINATES

θ_N : angle of rotation of the neck from the vertical about point O.

ϕ_N : angle of rotation of the neck from the line of the body midsagittal plane about point O.

θ_H : angle of rotation of the head from the vertical about point P.

ϕ_H : angle of rotation of the head from the body midsagittal plane about point P.

CONSTRAINT COORDINATES

l_N : length from O to mass of neck.

L_N : length of neck rod from O to P.

L_H : length of head rod from P to mass of head/helmet.

x : position relative to inertial frame; positive direction is face out.

y : position relative to inertial frame; positive direction is to body left.

z : position relative to inertial frame; positive direction is up.

CONSTANTS

m_N : mass of neck

m_H : combined mass of head and helmet

I_{ij}^K : combined head and helmet inertial properties calculated about the head/helmet center-of-gravity.

K: rotation location (O or P)

i, j: axes

β_c : rotational spring stiffnesses in the directions noted by c.

c: θ_N, θ_H, ϕ_N, ϕ_H

θ_{NO} : initial deflection of neck in the θ_N direction

ϕ_{NO} : initial deflection of neck in the ϕ_N direction

θ_{HO} : initial deflection of neck in the θ_H direction

ϕ_{HO} : initial deflection of neck in the ϕ_H direction

SPECIAL NOTATIONS

(A) Initial positions and deflections:

$$\Theta_N = \theta_N + \theta_{NO} \qquad \Theta_H = \theta_H + \theta_{HO}$$

$$\Phi_N = \phi_N + \phi_{NO} \qquad \Phi_H = \phi_H + \phi_{HO}$$

These expressions reflected both the direction and initial deflection of the neck and head/helmet masses. For simplicity, the capital notations (Θ_N, Φ_N, Θ_H, Φ_H) were used in the development, until expansion was required for clarity.

(B) Point locations:

O : support point for system; corresponds to C7-T1 vertebral position of the human neck.

N : location of neck mass.

P : location of head pivot; located near C1 vertebra of human neck.

H : location of head/helmet center-of-gravity.

CONSIDERATION OF COORDINATE SYSTEMS

(A) **[X,Y,Z]** was an inertial frame of reference with origin **U**. The position of O was represented at any time by $(X,Y,Z)_O$. Its initial position was denoted by $(X_o,Y_o,Z_o)_O$. Movement of O was represented by **x(t)** in the **X** direction, **y(t)** in the **Y** direction, and **z(t)** in the **Z** direction. From these definitions, $(X,Y,Z)_O$ was expressed in terms of its initial position $(X_O, Y_O, Z_O)_O$ and its translation x(t), y(t), and z(t); that is,

$$(X)_O = (X_O)_O + x(t)$$

$$(Y)_O = (Y_O)_O + y(t)$$

$$(Z)_O = (Z_O)_O + z(t)$$

Also, any other member of the O coordinate frame could be found in relation to the inertial system.

(B) [x,y,z] was the moving coordinate frame with origin at O and with its respective axes parallel to the inertial frame [X,Y,Z]. In addition, points **N**, **P**, and **H** were defined in this frame:

$$\mathbf{N} : (x_N, y_N, z_N)$$

$$\mathbf{P} : (x_P, y_P, z_P)$$

$$\mathbf{H} : (x_H, y_H, z_H)$$

Motion important to this analysis was confined to and interacted with this coordinate frame.

(C) The length of the rods connecting the pivot at the origin O with the neck mass at **N**, the pivot at O with the pivot at **P**, and the pivot at **P** with the head/helmet mass at **H** (l_N, L_{ON}, L_H, respectively) were each held constant, thus representing scleronomic constraints (they did not change with time). Therefore, these lengths could be represented by the expressions,

$$l_N{}^2 = x_N{}^2 + y_N{}^2 + z_N{}^2$$

$$L_N{}^2 = x_P{}^2 + y_P{}^2 + z_P{}^2$$

$$L_H{}^2 = (x_H - x_P)^2 + (y_H - y_P)^2 + (z_H - z_P)^2$$

In terms of the generalized coordinates θ_N, θ_H, ϕ_N, and ϕ_H (using the expressions Θ_N, Φ_N, Θ_H, and Φ_H as defined earlier), the expressions for the positions of N, P, and H were redefined as

$$\begin{aligned}
\text{N:}\quad x_N &= l_N \sin\Theta_N \cos\Phi_N \\
y_N &= l_N \sin\Theta_N \sin\Phi_N \\
z_N &= l_N \cos\Theta_N \\
\text{P:}\quad x_P &= L_N \sin\Theta_N \cos\Phi_N \\
y_P &= L_N \sin\Theta_N \sin\Phi_N \\
z_P &= L_N \cos\Theta_N \\
\text{H:}\quad x_H &= L_N \sin\Theta_N \cos\Phi_N + L_H \sin\Theta_H \cos\Phi_H \\
y_H &= L_N \sin\Theta_N \sin\Phi_N + L_H \sin\Theta_H \sin\Phi_H \\
z_H &= L_N \cos\Theta_N + L_H \cos\Theta_H
\end{aligned}$$

This formulation yielded a four degree of freedom system expressed in four generalized coordinates.

MOVING CONSTRAINTS

$x(t)$, $y(t)$, and $z(t)$ were specified as functions defining movement of the O coordinate frame. A convenient example of this motion corresponding to the vibratory motion studied in the physical tests was

$$x(t) = A_x \sin\Omega t \qquad y(t) = A_y \sin\Omega t$$

$$z(t) = A_z \sin\Omega t$$

where A_x, A_y, and A_z are amplitude multipliers.

Introduction of these moving constraints makes the system non-conservative, by definition. Typically, the Lagrangian approach is reserved for conservative systems, but these constraint motions, or "forces", act through the origin O and do not contribute to the generalized forces Q_θ and Q_Φ (which include the potential energy for the system). Therefore, the basic form of Lagrange's equation is applicable (Greenwood, 1965).

DEVELOPMENT OF EQUATIONS OF MOTION USING LAGRANGE'S EQUATION

Lagrange's Equation (standard form):

$$\frac{d}{dt}\left[\frac{\delta \pounds}{\delta \dot{q}_i}\right] - \frac{\delta \pounds}{\delta q_i} = 0$$

where $\pounds = T - V$,

T is the system kinetic energy,

V is the system potential energy,

q_i represents the generalized coordinates for the system.

(A) System Kinetic Energy

$$T = \tfrac{1}{2} \left(\Sigma\, m_i\, v_i^2 + \Sigma\, I\, \Omega^2 \right)$$

where m_i represents the individual masses,

v_i represents the individual velocities,

I represents the mass moment of inertia for the system,

Ω represents the angular velocity.

Expanding this expression including each term,

$$T = \tfrac{1}{2}\, m_N\, V_N^2 + \tfrac{1}{2}[I_N]\ \{\Omega\}_N + \tfrac{1}{2}\, m_H\, V_H^2$$
$$+ \{\Omega\}_N^T\ [I_H]^O\ \{\Omega\}_N$$
$$+ \{\Omega\}_H^T\ [I_H]^P\ \{\Omega\}_H$$

For this development,

$$[I_N] = \begin{bmatrix} 0 & 0 & 0 \\ 0 & 0 & 0 \\ 0 & 0 & 0 \end{bmatrix}$$

$$[I_H] = \begin{bmatrix} I_{xx} & -I_{xy} & -I_{xz} \\ -I_{yx} & I_{yy} & -I_{yz} \\ -I_{zx} & -I_{zy} & I_{zz} \end{bmatrix}^{O\ (\text{or } P)}$$

$$\{\Omega\}_N = \begin{bmatrix} 0 \\ \dot{\theta}_N \\ \dot{\phi}_N \end{bmatrix} \qquad \{\Omega\}_H = \begin{bmatrix} 0 \\ \dot{\theta}_H \\ \dot{\phi}_H \end{bmatrix}$$

(1) Velocity

$$v_N : \quad \vec{v}_N = (\dot{x} + \dot{x}_N)\,\hat{i} + (\dot{y} + \dot{y}_N)\,\hat{j} + (\dot{z} + \dot{z}_N)\,\hat{k}$$

where $\dot{x}$, $\dot{y}$, $\dot{z}$ are motions of the O coordinate frame, and where

$$\dot{x}_N = l_N\,\dot{\theta}_N \cos\theta_N \cos\Phi_N - l_N\,\dot{\Phi}_N \sin\theta_N \sin\Phi_N$$
$$\dot{y}_N = l_N\,\dot{\theta}_N \cos\theta_N \sin\Phi_N - l_N\,\dot{\Phi}_N \sin\theta_N \cos\Phi_N$$
$$\dot{z}_N = -l_N\,\dot{\theta}_N \sin\theta_N$$

Now,

$$\begin{aligned} v_N^2 &= (\dot{x} + \dot{x}_N)^2 + (\dot{y} + \dot{y}_N)^2 + (\dot{z} + \dot{z}_N)^2 \\ &= \dot{x}^2 + 2\dot{x}\dot{x}_N + \dot{x}_N^2 + \dot{y}^2 + 2\dot{y}\dot{y}_N + \dot{y}_N^2 \\ &\quad + \dot{z}^2 + 2\dot{z}\dot{z}_N + \dot{z}_N^2 \\ &= \dot{x}^2 + \dot{y}^2 + \dot{z}^2 + 2(\dot{x}\dot{x}_N + \dot{y}\dot{y}_N + \dot{z}\dot{z}_N) \\ &\quad + \dot{x}_N^2 + \dot{y}_N^2 + \dot{z}_N^2 \end{aligned}$$

$$\begin{aligned} v_N^2 = {} & \dot{x}^2 + \dot{y}^2 + \dot{z}^2 \\ & + 2\, l_N\, [\dot{x}(\dot{\theta}_N\cos\theta_N\cos\Phi_N - \dot{\Phi}_N\sin\theta_N\sin\Phi_N) \\ & \qquad + \dot{y}(\dot{\theta}_N\cos\theta_N\sin\Phi_N + \dot{\Phi}_N\sin\theta_N\sin\Phi_N) \\ & \qquad\quad + \dot{z}(-\dot{\theta}_N\sin\theta_N)] \\ & + l_N^2\dot{\theta}_N^2\cos^2\theta_N\cos^2\Phi_N \\ & - 2\, l_N^2\dot{\theta}_N\dot{\Phi}_N\cos\theta_N\cos\Phi_N\sin\theta_N\sin\Phi_N \\ & + l_N^2\dot{\Phi}_N^2\sin^2\theta_N\sin^2\Phi_N \\ & + l_N^2\dot{\theta}_N^2\cos^2\theta_N\sin^2\Phi_N \\ & + 2\, l_N^2\dot{\theta}_N\dot{\Phi}_N\cos\theta_N\sin\Phi_N\sin\theta_N\cos\Phi_N \\ & + l_N^2\dot{\Phi}_N^2\sin^2\theta_N\cos^2\Phi_N + l_N^2\dot{\theta}_N^2\sin^2\theta_N \end{aligned}$$

Finally,

(I) v_N :

$$
\begin{aligned}
v_N{}^2 = {} & \dot{x}^2 + \dot{y}^2 + \dot{z}^2 \\
& + 2l_N\{\dot{\theta}_N[\cos\theta_N(\dot{x}\cos\Phi_N+\dot{y}\sin\Phi_N)-\dot{z}\sin\theta_N] \\
& \qquad + \dot{\Phi}_N[\sin\theta_N(-\dot{x}\sin\Phi_N+\dot{y}\cos\Phi_N)\} \\
& + l_N{}^2\,\dot{\theta}_N{}^2 + l_N{}^2\dot{\Phi}_N{}^2\sin^2\theta_N
\end{aligned}
$$

$\vec{v}_H$: $\vec{v}_H = (\dot{x} + \dot{x}_H)\,\hat{i} + (\dot{y} + \dot{y}_H)\,\hat{j} + (\dot{z} + \dot{z}_H)\,\hat{k}$

where $\dot{x}$, $\dot{y}$, $\dot{z}$ are motions of the O coordinate frame, and where

$$
\begin{aligned}
\dot{x}_N = {} & L_N\,\dot{\theta}_N\,\cos\theta_N\,\cos\Phi_N - L_N\,\dot{\Phi}_N\,\sin\theta_N\,\sin\Phi_N \\
& + L_H\,\dot{\theta}_H\,\cos\theta_H\,\cos\Phi_H - L_H\,\dot{\Phi}_H\,\sin\theta_H\,\sin\Phi_H \\
\dot{y}_N = {} & L_N\,\dot{\theta}_N\,\cos\theta_N\,\sin\Phi_N - L_N\,\dot{\Phi}_N\,\sin\theta_N\,\cos\Phi_N \\
& + L_H\,\dot{\theta}_H\,\cos\theta_H\,\sin\Phi_H - L_H\,\dot{\Phi}_H\,\sin\theta_H\,\cos\Phi_H \\
\dot{z}_N = {} & -L_N\,\dot{\theta}_N\,\sin\theta_N - L_H\,\dot{\theta}_H\,\sin\theta_H
\end{aligned}
$$

Now,

$$
\begin{aligned}
v_H{}^2 & = (\dot{x} + \dot{x}_H)^2 + (\dot{y} + \dot{y}_H)^2 + (\dot{z} + \dot{z}_H)^2 \\
& = \dot{x}^2 + 2\dot{x}\dot{x}_H + \dot{x}_H{}^2 + \dot{y}^2 + 2\dot{y}\dot{y}_H + \dot{y}_H{}^2 \\
& \quad + \dot{z}^2 + 2\dot{z}\dot{z}_H + \dot{z}_H{}^2 \\
& = \dot{x}^2 + \dot{y}^2 + \dot{z}^2 + 2(\dot{x}\dot{x}_H + \dot{y}\dot{y}_H + \dot{z}\dot{z}_H) \\
& \quad + \dot{x}_H{}^2 + \dot{y}_H{}^2 + \dot{z}_H{}^2
\end{aligned}
$$

$$
\begin{aligned}
v_H{}^2 = {} & \dot{x}^2 + \dot{y}^2 + \dot{z}^2 \\
& + 2\dot{x}(L_N\dot{\theta}_N\cos\theta_N\cos\Phi_N - L_N\dot{\Phi}_N\sin\theta_N\sin\Phi_N \\
& \qquad + L_H\dot{\theta}_H\cos\theta_H\cos\Phi_H - L_H\dot{\Phi}_H\sin\theta_H\sin\Phi_H) \\
& + 2\dot{y}(L_N\dot{\theta}_N\cos\theta_N\sin\Phi_N + L_N\dot{\Phi}_N\sin\theta_N\sin\Phi_N \\
& \qquad + L_H\dot{\theta}_H\cos\theta_H\sin\Phi_H + L_H\dot{\Phi}_H\sin\theta_H\sin\Phi_H) \\
& + 2\dot{z}(-L_N\dot{\theta}_N\sin\theta_N - L_H\dot{\theta}_H\sin\theta_H)
\end{aligned}
$$

$$+ L_N^2\dot{\theta}_N^2\cos^2\theta_N\cos^2\Phi_N$$
$$- 2\ L_N^2\dot{\theta}_N\dot{\Phi}_N\cos\theta_N\cos\Phi_N\sin\theta_N\sin\Phi_N$$
$$+ 2\ L_N L_H\dot{\theta}_N\dot{\theta}_H\cos\theta_N\cos\Phi_N\cos\theta_H\cos\Phi_H$$
$$- 2\ L_N L_H\dot{\theta}_N\dot{\Phi}_H\cos\theta_N\cos\Phi_N\sin\theta_H\sin\Phi_H$$
$$+ L_N^2\dot{\Phi}_N^2\sin^2\theta_N\sin^2\Phi_N$$
$$- 2\ L_N L_H\dot{\Phi}_N\dot{\theta}_H\sin\theta_N\sin\Phi_N\cos\theta_H\cos\Phi_H$$
$$+ 2\ L_N L_H\dot{\Phi}_N\dot{\Phi}_H\sin\theta_N\sin\Phi_N\sin\theta_H\sin\Phi_H$$
$$+ L_H^2\dot{\theta}_H^2\cos^2\theta_H\cos^2\Phi_H$$
$$- 2\ L_H^2\dot{\theta}_H\dot{\Phi}_H\cos\theta_H\cos\Phi_H\sin\theta_H\sin\Phi_H$$
$$+ L_H^2\dot{\Phi}_H^2\sin^2\theta_H\sin^2\Phi_H$$
$$+ L_N^2\dot{\theta}_N^2\cos^2\theta_N\sin^2\Phi_N$$
$$+ 2\ L_N^2\dot{\theta}_N\dot{\Phi}_N\cos\theta_N\sin\Phi_N\sin\theta_N\cos\Phi_N$$
$$+ 2\ L_N L_H\dot{\theta}_N\dot{\theta}_H\cos\theta_N\sin\Phi_N\cos\theta_H\sin\Phi_H$$
$$+ 2\ L_N L_H\dot{\theta}_N\dot{\Phi}_H\cos\theta_N\sin\Phi_N\sin\theta_H\cos\Phi_H$$
$$+ L_N^2\dot{\Phi}_N^2\sin^2\theta_N\cos^2\Phi_N$$
$$+ 2\ L_N L_H\dot{\Phi}_N\dot{\theta}_H\sin\theta_N\cos\Phi_N\cos\theta_H\sin\Phi_H$$
$$+ 2\ L_N L_H\dot{\Phi}_N\dot{\Phi}_H\sin\theta_N\cos\Phi_N\sin\theta_H\cos\Phi_H$$
$$+ L_H^2\dot{\theta}_H^2\cos^2\theta_H\sin^2\Phi_H$$
$$+ 2\ L_H^2\dot{\theta}_H\Phi_H\cos\theta_H\sin\Phi_H\sin\theta_H\cos\Phi_H$$
$$+ L_H^2\dot{\Phi}_H^2\sin^2\theta_H\cos^2\Phi_H$$
$$+ L_N^2\dot{\theta}_N^2\sin^2\theta_N$$
$$+ 2\ L_N L_H\dot{\theta}_N\dot{\theta}_H\sin\theta_N\sin\theta_H + L_H^2\dot{\theta}_H^2\sin^2\theta_H$$

$$v_H^2 = \dot{x}^2 + \dot{y}^2 + \dot{z}^2$$
$$+ 2L_N\dot{\theta}_N[\cos\theta_N(\dot{x}\cos\Phi_N + \dot{y}\sin\Phi_N) - \dot{z}\sin\theta_N]$$
$$+ 2L_N\dot{\Phi}_N[\sin\theta_N(-\dot{x}\sin\Phi_N + \dot{y}\cos\Phi_N)]$$
$$+ 2L_H\dot{\theta}_H[\cos\theta_H(\dot{x}\cos\Phi_H + \dot{y}\sin\Phi_H) - \dot{z}\sin\theta_H]$$
$$+ 2L_H\dot{\Phi}_H[\sin\theta_H(-\dot{x}\sin\Phi_H + \dot{y}\cos\Phi_H)]$$
$$+ L_N^2\dot{\theta}_N^2$$
$$+ 2\ L_N L_H\dot{\theta}_N\dot{\theta}_H\cos\theta_N\cos\theta_H(\cos\Phi_N\cos\Phi_H + \sin\Phi_N\sin\Phi_H)$$
$$+ L_N^2\dot{\Phi}_N^2\sin^2\theta_N$$
$$+ 2\ L_N L_H\dot{\Phi}_N\dot{\theta}_H\sin\theta_N\cos\theta_H(-\sin\Phi_N\cos\Phi_H + \cos\Phi_N\sin\Phi_H)$$

$$+\ 2\,L_N L_H \dot{\Phi}_N \dot{\Phi}_H \sin\Theta_N \sin\Theta_H (\sin\Phi_N \sin\Phi_H + \cos\Phi_N \cos\Phi_H)$$
$$+\ L_H^2 \dot{\Theta}_H^2 + L_H^2 \dot{\Phi}_H^2 \sin^2\Theta_H$$
$$+\ 2\,L_N L_H \dot{\Theta}_N \dot{\Theta}_H \sin\Theta_N \sin\Theta_H$$
$$+\ 2\,L_N L_H \dot{\Theta}_N \dot{\Phi}_H \cos\Theta_N \sin\Theta_H (\sin\Phi_N \cos\Phi_H - \cos\Phi_N \sin\Phi_H)$$

Finally,

(II) v_H :

$$
\begin{aligned}
v_H^2 = {} & \dot{x}^2 + \dot{y}^2 + \dot{z}^2 \\
& + 2L_N\dot{\Theta}_N[\cos\Theta_N(\dot{x}\cos\Phi_N + \dot{y}\sin\Phi_N) - \dot{z}\sin\Theta_N] \\
& + 2L_N\dot{\Phi}_N[\sin\Theta_N(-\dot{x}\sin\Phi_N + \dot{y}\cos\Phi_N)] \\
& + 2L_H\dot{\Theta}_H[\cos\Theta_H(\dot{x}\cos\Phi_H + \dot{y}\sin\Phi_H) - \dot{z}\sin\Theta_H] \\
& + 2L_H\dot{\Phi}_H[\sin\Theta_H(-\dot{x}\sin\Phi_H + \dot{y}\cos\Phi_H)] \\
& + L_N^2\dot{\Theta}_N^2 \\
& + 2\,L_N L_H \dot{\Theta}_N \dot{\Theta}_H \cos\Theta_N \cos\Theta_H \cos(\Phi_N - \Phi_H) \\
& + L_N^2 \dot{\Phi}_N^2 \sin^2\Theta_N \\
& + 2\,L_N L_H \dot{\Theta}_N \dot{\Phi}_H \cos\Theta_N \sin\Theta_H \sin(\Phi_N - \Phi_H) \\
& + 2\,L_N L_H \dot{\Phi}_N \dot{\Theta}_H \sin\Theta_N \cos\Theta_H \sin(\Phi_N - \Phi_H) \\
& + 2\,L_N L_H \dot{\Phi}_N \dot{\Phi}_H \sin\Theta_N \sin\Theta_H \cos(\Phi_N - \Phi_H) \\
& + L_H^2 \dot{\Theta}_H^2 \\
& + 2\,L_N L_H \dot{\Theta}_N \dot{\Theta}_H \sin\Theta_N \sin\Theta_H \\
& + L_H^2 \dot{\Phi}_H^2 \sin^2\Theta_H
\end{aligned}
$$

(2) Inertia

$$
[\ 0\ \ \dot{\Theta}_N\ \ \dot{\Phi}_N\ ]
\begin{bmatrix} I_{xx} & -I_{xy} & -I_{xz} \\ -I_{yx} & I_{yy} & -I_{yz} \\ -I_{zx} & -I_{zy} & I_{zz} \end{bmatrix}_H^{O}
\begin{bmatrix} 0 \\ \dot{\Theta}_N \\ \dot{\Phi}_N \end{bmatrix}
$$

(III) $$= I_{yy}^{O}\,\dot{\Theta}_N^2 - 2\,I_{yz}^{O}\,\dot{\Theta}_N\,\dot{\Phi}_N + I_{zz}^{O}\,\dot{\Phi}_N^2$$

$$[\,0\ \ \dot{\theta}_H\ \ \dot{\Phi}_H\,]\begin{bmatrix} I_{xx} & -I_{xy} & -I_{xz} \\ -I_{yx} & I_{yy} & -I_{yz} \\ -I_{zx} & -I_{zy} & I_{zz} \end{bmatrix}_H^P \begin{bmatrix} 0 \\ \dot{\theta}_H \\ \dot{\Phi}_H \end{bmatrix}$$

$$\text{(IV)} \qquad = I_{yy}^{o}\ \dot{\theta}_H^2 - 2\ I_{yz}^{o}\ \dot{\theta}_H\ \dot{\Phi}_H + I_{zz}^{o}\ \dot{\Phi}_H^2$$

(3) Summation of terms

Gathering terms from (I), (II), (III), and (IV), in the form

$$T = \tfrac{1}{2}\ m_N\ V_N^2 + \tfrac{1}{2}[I_N]\ \{\Omega\}_N + \tfrac{1}{2}\ m_H\ V_H^2$$
$$+ \{\Omega\}_N^T\ [I_H]^o\ \{\Omega\}_N + \{\Omega\}_H^T\ [I_H]^P\ \{\Omega\}_H$$

$$\begin{aligned}
T = {} & \tfrac{1}{2}\ (m_N + m_H)\ (x^2 + y^2 + z^2) \\
& + (m_N l_N + m_H L_H)\ \dot{\theta}_N\ [\cos\theta_N\ (\dot{x}\ \cos\Phi_N + \dot{y}\ \sin\Phi_N) - \dot{z}\ \sin\theta_N] \\
& + (m_N l_N + m_H L_N)\dot{\Phi}_N\ [\sin\theta_N\ (-\dot{x}\ \sin\Phi_N + \dot{y}\ \cos\Phi_N)] \\
& + \tfrac{1}{2}\ (m_N l_N^2 + m_H L_N^2)\ (\dot{\theta}_N^2 + \dot{\Phi}_N^2\ \sin^2\theta_N) \\
& + m_H L_H \dot{\theta}_H\ [\cos\theta_H\ (\dot{x}\ \cos\Phi_H + \dot{y}\ \sin\Phi_H) - \dot{z}\ \sin\theta_H] \\
& + m_H L_H \dot{\Phi}_H\ [\sin\theta_H\ (-\dot{x}\ \sin\Phi_H + \dot{y}\ \cos\Phi_H)] \\
& + m_H L_N L_H\ [\dot{\theta}_N \dot{\theta}_H\ \cos\theta_N\ \cos\theta_H\ \cos(\Phi_N - \Phi_H) \\
& \qquad + \dot{\Phi}_N \dot{\theta}_H\ \sin\theta_N\ \cos\theta_H\ \sin(\Phi_N - \Phi_H)] \\
& + m_H L_N L_H\ [\dot{\theta}_N \dot{\Phi}_H\ \cos\theta_N\ \sin\theta_H\ \cos(\Phi_N - \Phi_H) \\
& \qquad\qquad + \dot{\Phi}_N \dot{\Phi}_H\ \sin\theta_N\ \sin\theta_H\ \cos(\Phi_N - \Phi_H) \\
& \qquad\qquad + \dot{\theta}_N \dot{\theta}_H\ \sin\theta_N\ \sin\theta_H] \\
& + \tfrac{1}{2}\ m_H L_H^2\ (\dot{\theta}_H^2 + \dot{\Phi}_H^2\ \sin^2\theta_H) \\
& + \tfrac{1}{2}\ (I_{yy}^{o}\ \dot{\theta}_N^2 - 2\ I_{yz}^{o}\ \dot{\theta}_N \dot{\Phi}_N + I_{zz}^{o}\ \dot{\Phi}_N^2) \\
& + \tfrac{1}{2}\ (I_{yy}^{P}\ \dot{\theta}_H^2 - 2\ I_{yz}^{P}\ \dot{\theta}_H \dot{\Phi}_H + I_{zz}^{P}\ \dot{\Phi}_H^2)
\end{aligned}$$

(B) System Potential Energy

(1) Spring potential energy

The general equation for the spring potential energy for rotational springs was

$$V_s = \tfrac{1}{2} \Sigma\, k_i\, \alpha_i$$

where k_i is the stiffness of the spring,

α_i is the angle of deflection.

From this general form, the spring potential energy for the model was

$$V_s = \tfrac{1}{2}\, \beta_{\theta N}\, \theta_N^2 + \tfrac{1}{2}\, \beta_{\theta H}\, (\theta_H - \theta_N)^2$$
$$+ \tfrac{1}{2}\, \beta_{\Phi N}\, \Phi_N^2 + \tfrac{1}{2}\, \beta_{\Phi H}\, (\Phi_H - \Phi_N)^2$$

(2) Gravitational potential energy

The general form of the gravitational potential energy is

$$V_G = \Sigma\, m_i h_i g$$

where m_i is the individual mass,

h_i is the mass's height above the moving coordinate system,

g is the gravitational constant.

From this form, the gravitational potential energy for the system was

$$V_g = m_N\ g\ l_N\ \cos\theta_N + m_H\ g\ (L_N\ \cos\theta_N + L_H\ \cos\theta_H)$$
$$+ (m_H + m_N)\ g\ z_O$$

(3) Summation of terms

$$V = \tfrac{1}{2}\ \beta_{\theta N}\ \theta_N^2 + \tfrac{1}{2}\ \beta_{\theta H}\ (\theta_H - \theta_N)^2 + \tfrac{1}{2}\ \beta_{\Phi N}\ \Phi_N^2$$
$$+ \tfrac{1}{2}\ \beta_{\Phi H}\ (\Phi_H - \Phi_N)^2 + m_N\ g\ l_N\ \cos\theta_N$$
$$+ m_H\ g\ (L_N\ \cos\theta_N + L_H\ \cos\theta_H) + (m_H + m_N)\ g\ z_O$$

(C) Lagrangian Functional $\quad \pounds = T - V$

$$\pounds = \tfrac{1}{2}\ (m_N + m_H)\ (\dot{x}^2 + \dot{y}^2 + \dot{z}^2)$$
$$+ (m_N l_N + m_H L_N)\ \dot{\theta}_N\ [\cos\theta_N\ (\dot{x}\ \cos\Phi_N + \dot{y}\ \sin\Phi_N) - \dot{z}\ \sin\theta_N]$$
$$+ (m_N l_N + m_H L_N)\dot{\Phi}_N\ [\sin\theta_N\ (-\dot{x}\ \sin\Phi_N + \dot{y}\ \cos\Phi_N)]$$
$$+ \tfrac{1}{2}\ (m_N l_N^2 + m_H L_N^2)\ (\dot{\theta}_N^2 + \dot{\Phi}_N^2\ \sin^2\theta_N)$$
$$+ m_H L_H \dot{\theta}_H\ [\cos\theta_H\ (\dot{x}\ \cos\Phi_H + \dot{y}\ \sin\Phi_H) - \dot{z}\ \sin\theta_H]$$
$$+ m_H L_H \dot{\Phi}_H\ [\sin\theta_H\ (-\dot{x}\ \sin\Phi_H + \dot{y}\ \cos\Phi_H)]$$
$$+ m_H L_N L_H\ [\dot{\theta}_N \dot{\theta}_H\ \cos\theta_N\ \cos\theta_H\ \cos(\Phi_N - \Phi_H)$$
$$+ \dot{\Phi}_N \dot{\theta}_H\ \sin\theta_N\ \cos\theta_H\ \sin(\Phi_N - \Phi_H)]$$
$$+ m_H L_N L_H\ [\dot{\theta}_N \dot{\Phi}_H\ \cos\theta_N\ \sin\theta_H\ \cos(\Phi_N - \Phi_H)$$
$$+ \dot{\Phi}_N \dot{\Phi}_H\ \sin\theta_N\ \sin\theta_H\ \cos(\Phi_N - \Phi_H)$$
$$+ \dot{\theta}_N \dot{\theta}_H\ \sin\theta_N\ \sin\theta_H]$$

$$+ \tfrac{1}{2}\, m_H L_H^2\ (\dot{\theta}_H^2 + \dot{\Phi}_H^2 \sin^2\theta_H)$$

$$+ \tfrac{1}{2}\ (I_{YY}^{O}\ \dot{\theta}_N^2 - 2\ I_{YZ}^{O}\ \dot{\theta}_N\dot{\Phi}_N + I_{ZZ}^{O}\ \dot{\Phi}_N^2)$$

$$+ \tfrac{1}{2}\ (I_{YY}^{P}\ \dot{\theta}_H^2 - 2\ I_{YZ}^{P}\ \dot{\theta}_H\dot{\Phi}_H + I_{ZZ}^{P}\ \dot{\Phi}_H^2)$$

$$- \tfrac{1}{2}\ \beta_{\theta N}\ \theta_N^2 - \tfrac{1}{2}\ \beta_{\theta H}\ (\theta_H - \theta_N)^2 - \tfrac{1}{2}\ \beta_{\Phi N}\ \Phi_N^2$$

$$- \tfrac{1}{2}\ \beta_{\Phi H}\ (\Phi_H - \Phi_N)^2 - m_N\ g\ l_N\ \cos\theta_N$$

$$- m_H\ g\ (L_N \cos\theta_N + L_H \cos\theta_H) - (m_H + m_N)\ g\ z_O$$

(D) Evaluation of Lagrangian Equation

$$\frac{d}{dt}\left[\frac{\delta \pounds}{\delta \dot{q}_i}\right] - \frac{\delta \pounds}{\delta q_i} = 0$$

θ_N:

$$\frac{\delta \pounds}{\delta \dot{\theta}_N} =$$

$$\begin{aligned}
&(m_N l_N + m_H L_N)\ [\cos\theta_N(\dot{x}\cos\Phi_N + \dot{y}\sin\Phi_N) - \dot{z}\sin\theta_N] \\
&+ (m_N l_N^2 + m_H L_N^2)\dot{\theta}_N \\
&+ m_H L_N L_H\ [\dot{\theta}_H\cos\theta_N\cos\theta_H\cos(\Phi_N - \Phi_H) \\
&\qquad + \dot{\Phi}_H\cos\theta_N\sin\theta_H\sin(\Phi_N - \Phi_H) \\
&\qquad\qquad + \dot{\theta}_H\ \sin\theta_N\ \sin\theta_H] \\
&+ I_{YY}^{O}\ \dot{\theta}_N - I_{YZ}^{O}\ \dot{\Phi}_N
\end{aligned}$$

$$\frac{d}{dt}\left[\frac{\delta \pounds}{\delta \dot{\theta}_N}\right] =$$

$$\begin{aligned}
&(m_N l_N + m_H L_N)\ [-\dot{\theta}_N\sin\theta_N\ (\dot{x}\cos\Phi_N + \dot{y}\sin\Phi_N) \\
&\qquad + \ddot{x}\cos\theta_N\cos\Phi_N - \dot{\Phi}_N\ \dot{x}\ \cos\theta_N\sin\Phi_N \\
&\qquad + \ddot{y}\cos\theta_N\sin\Phi_N - \dot{\Phi}_N\dot{y}\cos\theta_N\cos\Phi_N \\
&\qquad\qquad - \ddot{z}\ \sin\theta_N - \dot{z}\dot{\theta}_N\ \cos\theta_N] \\
&+ (m_N l_N^2 + m_H L_N^2)\ddot{\theta}_N
\end{aligned}$$

$$
\begin{aligned}
+\ & m_H L_N L_H [\ddot{\theta}_H \cos\theta_N \cos\theta_H \cos(\Phi_N - \Phi_H) \\
& \quad - \dot{\theta}_H \dot{\theta}_N \sin\theta_N \cos\theta_H \cos(\Phi_N - \Phi_H) \\
& \quad - \dot{\theta}_H{}^2 \cos\theta_N \sin\theta_H \cos(\Phi_N - \Phi_H) \\
& \quad - \dot{\theta}_H (\dot{\Phi}_N - \dot{\Phi}_H) \cos\theta_N \cos\theta_H \sin(\Phi_N - \Phi_H) \\
& \quad + \ddot{\Phi}_H \cos\theta_N \sin\theta_H \sin(\Phi_N - \Phi_H) \\
& \quad - \dot{\theta}_N \dot{\Phi}_H \sin\theta_N \sin\theta_H \sin(\Phi_N - \Phi_H) \\
& \quad + \dot{\theta}_H \dot{\Phi}_H \cos\theta_N \cos\theta_H \sin(\Phi_N - \Phi_H) \\
& \quad + \dot{\Phi}_H (\dot{\Phi}_N - \dot{\Phi}_H) \cos\theta_N \sin\theta_H \cos(\Phi_N - \Phi_H) \\
& \quad + \ddot{\theta}_H \sin\theta_N \sin\theta_H + \dot{\theta}_H \dot{\theta}_N \cos\theta_N \sin\theta_H \\
& \qquad + \dot{\theta}_H{}^2 \sin\theta_N \cos\theta_H] \\
+\ & I_{YY}{}^{\circ}\, \ddot{\theta}_N - I_{YZ}{}^{\circ}\, \ddot{\Phi}_N
\end{aligned}
$$

$$
\frac{\delta \pounds}{\delta \theta_N} =
$$

$$
\begin{aligned}
& (m_N l_N + m_H L_N)\{\dot{\theta}_N[-\sin\theta_N(\dot{x}\cos\Phi_N + \dot{y}\sin\Phi_N) - \dot{z}\cos\theta_N] \\
& \qquad + \dot{\Phi}_N[\cos\theta_N\ (-\dot{x}\sin\Phi_N + \dot{y}\cos\Phi_N)]\} \\
& + (m_N l_N{}^2 + m_H L_N{}^2)\dot{\Phi}_N{}^2 \cos\theta_N \sin\theta_N \\
& + m_H L_N L_H\ [-\dot{\theta}_N \dot{\theta}_H \sin\theta_N \cos\theta_H \cos(\Phi_N - \Phi_H) \\
& \qquad + \dot{\Phi}_N \dot{\theta}_H \cos\theta_N \cos\theta_H \sin(\Phi_N - \Phi_H) \\
& \qquad - \dot{\theta}_N \dot{\Phi}_H \sin\theta_N \sin\theta_H \sin(\Phi_N - \Phi_H) \\
& \qquad + \dot{\Phi}_N \dot{\Phi}_H \cos\theta_N \sin\theta_H \cos(\Phi_N - \Phi_H) \\
& \qquad\quad + \dot{\theta}_N \dot{\theta}_H \cos\theta_N \sin\theta_H] \\
& - \beta_{\theta N}\ \theta_N + \beta_{\theta H}(\theta_H - \theta_N) \\
& + m_N g l_N \sin\theta_N + m_H g L_N \sin\theta_N
\end{aligned}
$$

$$
\begin{aligned}
\theta_N :\quad & (m_N l_N{}^2 + m_H L_N{}^2 + I_{YY}{}^{\circ})\ddot{\theta}_N - I_{YZ}{}^{\circ}\ddot{\Phi}_N \\
& + \{m_H L_N L_H\ [\cos\theta_N \cos\theta_H \cos(\Phi_N - \Phi_H) + \sin\theta_N \sin\theta_H]\}\ddot{\theta}_H \\
& + [m_H L_N L_H\ \cos\theta_N \sin\theta_H \sin(\Phi_N - \Phi_H)]\ddot{\Phi}_H \\
& - [(m_N l_N{}^2 + m_H L_N{}^2)\ \cos\theta_N \sin\theta_H]\dot{\Phi}_N{}^2 \\
& - [2\ m_H L_N L_H\ \cos\theta_N \cos\theta_H \sin(\Phi_N - \Phi_H)]\dot{\theta}_H \dot{\Phi}_N \\
& + [2\ m_H L_N L_H\ \cos\theta_N \cos\theta_H \sin(\Phi_N - \Phi_H)]\dot{\theta}_H \dot{\Phi}_H \\
& + \{m_H L_N L_H[-\cos\theta_N \sin\theta_H \cos(\Phi_N - \Phi_H) + \sin\theta_N \cos\theta_H]\}\dot{\theta}_H{}^2 \\
& - [m_H L_N L_H\ \cos\theta_N \sin\theta_H \cos(\Phi_N - \Phi_H)]\dot{\Phi}_H{}^2 \\
& + (\beta_{\theta N} + \beta_{\theta H})\theta_N - \beta_{\theta H}\theta_H
\end{aligned}
$$

$$+ (m_N l_N + m_H L_N)[\ddot{x}\cos\theta_N\cos\Phi_N + \ddot{y}\cos\theta_N\sin\Phi_N - (\ddot{z} + g)\sin\theta_N] = 0$$

ϕ_N:

$$\frac{\delta \pounds}{\delta \dot{\phi}_N} =$$

$$\begin{aligned}
&+ (m_N l_N + m_H L_N)\,[\sin\dot{\theta}_N\,(-x\,\sin\dot{\Phi}_N + y\,\cos\Phi_N)] \\
&+ (m_N l_N^2 + m_H L_N^2)\dot{\Phi}_N\,\sin^2\theta_N \\
&+ m_H L_N L_H\,[\dot{\theta}_H\,\sin\theta_N\,\cos\theta_H\,\sin(\Phi_N - \Phi_H) \\
&\qquad + \dot{\Phi}_H\,\sin\theta_N\,\sin\theta_H\,\cos(\Phi_N - \Phi_H)] \\
&+ I_{yz}^{o}\,\dot{\theta}_N - I_{zz}^{o}\,\dot{\Phi}_N
\end{aligned}$$

$$\frac{d}{dt}\left[\frac{\delta \pounds}{\delta \dot{\phi}_N}\right] =$$

$$\begin{aligned}
&(m_N l_N + m_H L_N)\,[\dot{\theta}_N\cos\theta_N\,(-\dot{x}\sin\Phi_N + \dot{y}\cos\Phi_N) \\
&\qquad - \ddot{x}\sin\theta_N\sin\Phi_N - \dot{\Phi}_N\,\dot{x}\,\sin\theta_N\cos\Phi_N \\
&\qquad + \ddot{y}\sin\theta_N\cos\Phi_N - \dot{\Phi}_N\,\dot{y}\,\sin\theta_N\sin\Phi_N] \\
&+ 2(m_N l_N^2 + m_H L_N^2)\dot{\Phi}_N\dot{\theta}_N\,\sin\theta_N\cos\theta_N \\
&+ m_H L_N L_H[\ddot{\theta}_H\sin\theta_N\cos\theta_H\cos(\Phi_N-\Phi_H) \\
&\qquad + \dot{\theta}_H\dot{\theta}_N\cos\theta_N\cos\theta_H\sin(\Phi_N-\Phi_H) \\
&\qquad - \dot{\theta}_H^2\sin\theta_N\sin\theta_H\sin(\Phi_N-\Phi_H) \\
&\qquad + \dot{\theta}_H(\dot{\Phi}_N-\dot{\Phi}_H)\sin\theta_N\cos\theta_H\cos(\Phi_N-\Phi_H) \\
&\qquad + \ddot{\Phi}_H\sin\theta_N\sin\theta_H\cos(\Phi_N-\Phi_H) \\
&\qquad + \dot{\theta}_N\dot{\Phi}_H\cos\theta_N\sin\theta_H\cos(\Phi_N-\Phi_H) \\
&\qquad + \dot{\theta}_H\dot{\Phi}_H\sin\theta_N\cos\theta_H\cos(\Phi_N-\Phi_H) \\
&\qquad - \dot{\Phi}_H(\dot{\Phi}_N-\dot{\Phi}_H)\sin\theta_N\sin\theta_H\sin(\Phi_N-\Phi_H)] \\
&+ I_{yz}^{o}\,\ddot{\theta}_N - I_{zz}^{o}\,\ddot{\Phi}_N
\end{aligned}$$

$$\frac{\delta \pounds}{\delta \phi_N} =$$

$$\begin{aligned}
&(m_N l_N + m_H L_N)[\dot{\theta}_N\cos\theta_N(-\dot{x}\sin\Phi_N + \dot{y}\cos\Phi_N) \\
&\qquad + \dot{\Phi}_N\sin\theta_N\,(\dot{x}\cos\Phi_N + \dot{y}\sin\Phi_N)]
\end{aligned}$$

$$+ m_H L_N L_H \,[-\dot{\theta}_N \dot{\theta}_H \cos\theta_N \cos\theta_H \sin(\Phi_N - \Phi_H)$$
$$+ \dot{\Phi}_N \dot{\theta}_H \sin\theta_N \cos\theta_H \cos(\Phi_N - \Phi_H)$$
$$+ \dot{\theta}_N \dot{\Phi}_H \cos\theta_N \sin\theta_H \cos(\Phi_N - \Phi_H)$$
$$- \dot{\Phi}_N \dot{\Phi}_H \sin\theta_N \sin\theta_H \sin(\Phi_N - \Phi_H)]$$
$$- \beta_{\Phi N}\, \Phi_N + \beta_{\Phi H}(\Phi_H - \Phi_N)$$

$$\Phi_N :\quad - I_{YZ}{}^{O}\ddot{\theta}_N + [(m_N l_N{}^2 + m_H L_N{}^2)\sin^2\theta_N + I_{ZZ}{}^{O}]\ddot{\Phi}_N$$
$$+ [m_H L_N L_H \,\sin\theta_N \cos\theta_H \sin(\Phi_N - \Phi_H)]\ddot{\theta}_H$$
$$+ [m_H L_N L_H \,\sin\theta_N \sin\theta_H \cos(\Phi_N - \Phi_H)]\ddot{\Phi}_H$$
$$+ [2\ (m_N l_N{}^2 + m_H L_N{}^2)\sin\theta_N \cos\theta_H]\dot{\theta}_N \dot{\Phi}_N$$
$$- [m_H L_N L_H \,\sin\theta_N \sin\theta_H \sin(\Phi_N - \Phi_H)]\dot{\theta}_H{}^2$$
$$+ [m_H L_N L_H \,\sin\theta_N \sin\theta_H \sin(\Phi_N - \Phi_H)]\dot{\Phi}_H{}^2$$
$$+ (\beta_{\Phi N} + \beta_{\Phi H})\Phi_N - \beta_{\Phi H}\Phi_H$$
$$+ (m_N l_N + m_H L_N)\ (-\ddot{x}\ \sin\theta_N \sin\Phi_N + \ddot{y}\ \sin\theta_N \cos\Phi_N) = 0$$

θ_H:

$$\frac{\delta \pounds}{\delta \dot{\theta}_H} =$$

$$+ m_H L_H\, [\cos\theta_H\ (\dot{x}\ \cos\Phi_H + \dot{y}\ \sin\Phi_H) - \dot{z}\ \sin\theta_H]$$
$$+ m_H L_N L_H\, [\dot{\theta}_N\ \cos\theta_N\ \cos\theta_H\ \cos(\Phi_N - \Phi_H)$$
$$+ \dot{\Phi}_N\ \cos\theta_N\ \sin\theta_H\ \sin(\Phi_N - \Phi_H)$$
$$+ \dot{\theta}_N\ \sin\theta_N\ \sin\theta_H]$$
$$+ m_H L_H{}^2 \dot{\theta}_H + I_{YY}{}^{P}\ \dot{\theta}_H - I_{YZ}{}^{P}\ \dot{\Phi}_H$$

$$\frac{d}{dt}\left[\frac{\delta \pounds}{\delta \dot{\theta}_H}\right] =$$

$$m_H L_H\, [-\dot{\theta}_H \sin\theta_N\ (\dot{x}\cos\Phi_H + \dot{y}\sin\Phi_H)$$
$$+ \ddot{x}\cos\theta_H \cos\Phi_H - \dot{\Phi}_H\ \dot{x}\ \cos\theta_H \sin\Phi_H$$
$$+ \ddot{y}\cos\theta_H \sin\Phi_H - \dot{\Phi}_H\ \dot{y}\ \cos\theta_H \cos\Phi_H$$
$$- \ddot{z}\ \sin\theta_H - \dot{z}\ \dot{\theta}_H\ \cos\theta_H]$$

$$
\begin{aligned}
+\ m_H L_N L_H [&\ddot{\theta}_N \cos\theta_N \cos\theta_H \cos(\Phi_N-\Phi_H) \\
&- \dot{\theta}_N^2 \sin\theta_N \cos\theta_H \cos(\Phi_N-\Phi_H) \\
&- \dot{\theta}_H \dot{\theta}_N \cos\theta_N \sin\theta_H \cos(\Phi_N-\Phi_H) \\
&- \dot{\theta}_N (\dot{\Phi}_N-\dot{\Phi}_H) \cos\theta_N \cos\theta_H \sin(\Phi_N-\Phi_H) \\
&+ \ddot{\Phi}_N \sin\theta_N \cos\theta_H \sin(\Phi_N-\Phi_H) \\
&+ \dot{\theta}_N \dot{\Phi}_N \cos\theta_N \cos\theta_H \sin(\Phi_N-\Phi_H) \\
&- \dot{\theta}_H \dot{\Phi}_N \sin\theta_N \sin\theta_H \sin(\Phi_N-\Phi_H) \\
&+ \dot{\Phi}_N (\dot{\Phi}_N-\dot{\Phi}_H) \sin\theta_N \cos\theta_H \cos(\Phi_N-\Phi_H) \\
&+ \ddot{\theta}_N \sin\theta_N \sin\theta_H + \dot{\theta}_H \dot{\theta}_N \sin\theta_N \cos\theta_H \\
&\qquad\qquad + \dot{\theta}_N^2 \cos\theta_N \sin\theta_H] \\
+\ m_H L_H^2 \ddot{\theta}_H &+ I_{YY}^P\ \ddot{\theta}_H - I_{YZ}^P\ \ddot{\Phi}_H
\end{aligned}
$$

$$
\frac{\delta \pounds}{\delta \theta_H} =
$$

$$
\begin{aligned}
m_H L_H\ \{&\dot{\theta}_H[-\sin\theta_H(\dot{x}\cos\Phi_H + \dot{y}\sin\Phi_H) - \dot{z}\cos\theta_H] \\
&\qquad + \dot{\Phi}_H[\cos\theta_H\ (-\dot{x}\sin\Phi_H + \dot{y}\cos\Phi_H)]\} \\
+\ m_H L_N L_H\ [&-\dot{\theta}_N \dot{\theta}_H \cos\theta_N \sin\theta_H \cos(\Phi_N-\Phi_H) \\
&- \dot{\Phi}_N \dot{\theta}_H \sin\theta_N \sin\theta_H \sin(\Phi_N-\Phi_H) \\
&+ \dot{\theta}_N \dot{\Phi}_H \cos\theta_N \cos\theta_H \sin(\Phi_N-\Phi_H) \\
&+ \dot{\Phi}_N \dot{\Phi}_H \sin\theta_N \cos\theta_H \cos(\Phi_N-\Phi_H) \\
&\qquad + \dot{\theta}_N \dot{\theta}_H \sin\theta_N \cos\theta_H] \\
+\ m_H L_H^2 &\dot{\Phi}_H^2 \cos\theta_H \sin\theta_H \\
-\ \beta_{\theta H}&(\theta_H - \theta_N) + m_H g L_N \sin\theta_N
\end{aligned}
$$

$$
\begin{aligned}
\theta_H\ :\quad &\{m_H L_N L_H\ [\cos\theta_N \cos\theta_H \cos(\Phi_N-\Phi_H) + \sin\theta_N \sin\theta_H]\}\ddot{\theta}_N \\
&+ [m_H L_N L_H\ \sin\theta_N \cos\theta_H \sin(\Phi_N-\Phi_H)]\ddot{\Phi}_N \\
&+ (m_H L_H^2 + I_{YY}^P)\ddot{\theta}_H - I_{YZ}^P \ddot{\Phi}_H \\
&- [2\ m_H L_N L_H \sin\theta_N \cos\theta_H \cos(\Phi_N-\Phi_H)]\dot{\Phi}_N \dot{\Phi}_H \\
&+ \{m_H L_N L_H\ [-\sin\theta_N \cos\theta_H \cos(\Phi_N-\Phi_H) + \cos\theta_N \sin\theta_H]\}\dot{\theta}_N^2 \\
&+ [m_H L_N L_H\ \sin\theta_N \cos\theta_H \cos(\Phi_N-\Phi_H)]\dot{\Phi}_N^2
\end{aligned}
$$

$$- [m_H L_H^2 \cos\theta_N \sin\theta_H]\dot{\Phi}_H^2 - \beta_{eH}\theta_N + \beta_{eH}\theta_H$$

$$+ m_H L_H [\ddot{x} \cos\theta_H \cos\Phi_H + \ddot{y} \cos\theta_H \sin\Phi_H$$

$$- (\ddot{z} + g)\sin\theta_H] = 0$$

ϕ_H:

$$\frac{\delta \pounds}{\delta \dot{\phi}_H} =$$

$$m_H L_H [\sin\theta_H (-\dot{x} \sin\Phi_H + \dot{y} \cos\Phi_H)]$$

$$+ m_H L_N L_H [\dot{\theta}_N \cos\theta_N \sin\theta_H \sin(\Phi_N - \Phi_H)$$

$$+ \dot{\Phi}_N \sin\theta_N \sin\theta_H \cos(\Phi_N - \Phi_H)]$$

$$+ m_H L_H^2 \dot{\Phi}_N \sin^2\theta_N - I_{yz}^P \dot{\theta}_H + I_{zz}^P \dot{\Phi}_H$$

$$\frac{d}{dt}\left[\frac{\delta \pounds}{\delta \dot{\phi}_H}\right] =$$

$$m_H L_H [\dot{\theta}_H \cos\theta_H (-\dot{x}\sin\Phi_H + \dot{y}\cos\Phi_H)$$

$$-\ddot{x}\sin\theta_N\sin\Phi_N - \dot{\Phi}_H \dot{x} \sin\theta_N\cos\Phi_N$$

$$+\ddot{y}\sin\theta_N\cos\Phi_N - \dot{\Phi}_H \dot{y} \sin\theta_N\sin\Phi_N]$$

$$+ m_H L_N L_H[\ddot{\theta}_N\cos\theta_N\sin\theta_H\sin(\Phi_N-\Phi_H)$$

$$+ \dot{\theta}_H\dot{\theta}_N\cos\theta_N\cos\theta_H\sin(\Phi_N-\Phi_H)$$

$$- \dot{\theta}_N^2\sin\theta_N\sin\theta_H\sin(\Phi_N-\Phi_H)$$

$$+ \dot{\theta}_N(\dot{\Phi}_N-\dot{\Phi}_H)\cos\theta_N\sin\theta_H\cos(\Phi_N-\Phi_H)$$

$$+ \ddot{\Phi}_N\sin\theta_N\sin\theta_H\cos(\Phi_N-\Phi_H)$$

$$+ \dot{\theta}_N\dot{\Phi}_N\cos\theta_N\sin\theta_H\cos(\Phi_N-\Phi_H)$$

$$+ \dot{\theta}_H\dot{\Phi}_N\sin\theta_N\cos\theta_H\cos(\Phi_N-\Phi_H)$$

$$- \dot{\Phi}_N(\dot{\Phi}_N-\dot{\Phi}_H)\sin\theta_N\sin\theta_H\sin(\Phi_N-\Phi_H)]$$

$$+ 2m_H L_H^2\dot{\Phi}_H\dot{\theta}_H \sin\theta_H\cos\theta_H$$

$$- I_{yz}^P \ddot{\theta}_H + I_{zz}^P \ddot{\Phi}_H$$

$$\frac{\delta \pounds}{\delta \phi_H} =$$

$$
\begin{aligned}
& m_H L_H [\dot{\theta}_H \cos\theta_H(-\dot{x}\sin\Phi_H + \dot{y}\cos\Phi_H) \\
& \qquad\qquad + \dot{\Phi}_H \sin\theta_H \; (-\dot{x}\cos\Phi_H - \dot{y}\sin\Phi_H)] \\
& + m_H L_N L_H \; [\dot{\theta}_N\dot{\theta}_H \cos\theta_N \cos\theta_H \sin(\Phi_N - \Phi_H) \\
& \qquad - \dot{\Phi}_N\dot{\theta}_H \sin\theta_N \cos\theta_H \cos(\Phi_N - \Phi_H) \\
& \qquad - \dot{\theta}_N\dot{\Phi}_H \cos\theta_N \sin\theta_H \cos(\Phi_N - \Phi_H) \\
& \qquad + \dot{\Phi}_N\dot{\Phi}_H \sin\theta_N \sin\theta_H \sin(\Phi_N - \Phi_H)] \\
& + \beta_{\Phi H}(\Phi_H - \Phi_N)
\end{aligned}
$$

$$
\begin{aligned}
\phi_H : \quad & [m_H L_N L_H \; \cos\theta_N \sin\theta_H \sin(\Phi_N - \Phi_H)]\ddot{\theta}_N \\
& + [m_H L_N L_H \; \sin\theta_N \sin\theta_H \cos(\Phi_N - \Phi_H)]\ddot{\Phi}_N \\
& - I_{yz}{}^{P}\theta_H - (m_H L_H{}^2 \sin^2\theta_H + I_{zz}{}^{P})\Phi_H \\
& - [m_H L_N L_H \; \sin\theta_N \sin\theta_H \sin(\Phi_N - \Phi_H)]\theta_N{}^2 \\
& - [m_H L_N L_H \; \sin\theta_N \sin\theta_H \sin(\Phi_N - \Phi_H)]\Phi_N{}^2 \\
& + [2 \; m_H L_N L_H \; \cos\theta_N \sin\theta_H \cos(\Phi_N - \Phi_H)]\theta_N \Phi_N \\
& + [2 \; m_H L_N L_H \; \sin\theta_N \cos\theta_H \cos(\Phi_N - \Phi_H)]\theta_H \Phi_N \\
& - [2 \; m_H L_H{}^2 \; \sin\theta_N \cos\theta_H]\theta_H \Phi_H - \beta_{\Phi H}\Phi_N + \beta_{\Phi H}\Phi_H \\
& + m_H L_H \; (-\ddot{x} \; \cos\theta_H \cos\Phi_H + \ddot{y} \; \cos\theta_H \sin\Phi_H) = 0
\end{aligned}
$$

APPENDIX B

LINEARIZATION OF NONLINEAR EQUATION SYSTEM

(A) Neglect second and higher order terms.

$$
\begin{aligned}
\theta_N :\quad & (m_N l_N^2 + m_H L_N^2 + I_{YY}^O)\ddot{\theta}_N - I_{YZ}^O \ddot{\Phi}_N \\
& + \{m_H L_N L_H\, [\cos\theta_N \cos\theta_H \cos(\Phi_N - \Phi_H) + \sin\theta_N \sin\theta_H]\}\ddot{\theta}_H \\
& + [m_H L_N L_H\, \cos\theta_N \sin\theta_H \sin(\Phi_N - \Phi_H)]\ddot{\Phi}_H \\
& + (\beta_{\theta N} + \beta_{\theta H})\theta_N - \beta_{\theta H}\theta_H \\
& + (m_N l_N + m_H L_N)[\ddot{x}\cos\theta_N \cos\Phi_N + \ddot{y}\cos\theta_N \sin\Phi_N \\
& \qquad - (\ddot{z} + g)\sin\theta_N] = 0
\end{aligned}
$$

$$
\begin{aligned}
\Phi_N :\quad & - I_{YZ}^O \ddot{\theta}_N + [(m_N l_N^2 + m_H L_N^2)\sin^2\theta_N + I_{ZZ}^O]\ddot{\Phi}_N \\
& + [m_H L_N L_H\, \sin\theta_N \cos\theta_H \sin(\Phi_N - \Phi_H)]\ddot{\theta}_H \\
& + [m_H L_N L_H\, \sin\theta_N \sin\theta_H \cos(\Phi_N - \Phi_H)]\ddot{\Phi}_H \\
& + (\beta_{\Phi N} + \beta_{\Phi H})\Phi_N - \beta_{\Phi H}\Phi_H \\
& + (m_N l_N + m_H L_N)\ (-\ddot{x}\ \sin\theta_N \sin\Phi_N + \ddot{y}\ \sin\theta_N \cos\Phi_N) = 0
\end{aligned}
$$

$$
\begin{aligned}
\theta_H :\quad & \{m_H L_N L_H\, [\cos\theta_N \cos\theta_H \cos(\Phi_N - \Phi_H) + \sin\theta_N \sin\theta_H]\}\ddot{\theta}_N \\
& + [m_H L_N L_H\, \sin\theta_N \cos\theta_H \sin(\Phi_N - \Phi_H)]\ddot{\Phi}_N \\
& + (m_H L_H^2 + I_{YY}^P)\ddot{\theta}_H - I_{YZ}^P \ddot{\Phi}_H - \beta_{\theta H}\theta_N + \beta_{\theta H}\theta_H \\
& + m_H L_H\ [\ddot{x}\ \cos\theta_H \cos\Phi_H + \ddot{y}\ \cos\theta_H \sin\Phi_H \\
& \qquad - (\ddot{z} + g)\sin\theta_H] = 0
\end{aligned}
$$

$$
\begin{aligned}
\Phi_H :\quad & [m_H L_N L_H\, \cos\theta_N \sin\theta_H \sin(\Phi_N - \Phi_H)]\ddot{\theta}_N \\
& + [m_H L_N L_H\, \sin\theta_N \sin\theta_H \cos(\Phi_N - \Phi_H)]\ddot{\Phi}_N \\
& - I_{YZ}^P \ddot{\theta}_H - (m_H L_H^2 \sin^2\theta_H + I_{ZZ}^P)\ddot{\Phi}_H - \beta_{\Phi H}\Phi_N + \beta_{\Phi H}\Phi_H \\
& + m_H L_H\ (-\ddot{x}\ \cos\theta_H \cos\Phi_H + \ddot{y}\ \cos\theta_H \sin\Phi_H) = 0
\end{aligned}
$$

(B) Small Angle Approximation

Assume angles are small, such that for any small angles α and μ:

$$\cos\alpha \approx 1 \qquad \sin\mu \approx \mu \qquad |\alpha - \mu| \approx 0$$

Recall that

$$\Theta_N = \theta_N + \theta_{NO} \qquad \Theta_H = \theta_H + \theta_{HO}$$

$$\Phi_N = \phi_N + \phi_{NO} \qquad \Phi_H = \phi_H + \phi_{HO}$$

Assuming small angles, the following substitutions can be made:

$$\cos\Theta_N = \cos(\theta_N + \theta_{NO}) = \cos\theta_{NO}\cos\theta_N - \sin\theta_{NO}\sin\theta_N$$
$$\approx \cos\theta_{NO} - \theta_N \sin\theta_{NO}$$

$$\sin\Theta_N = \sin(\theta_N + \theta_{NO}) = \sin\theta_{NO}\cos\theta_N - \cos\theta_{NO}\sin\theta_N$$
$$\approx \sin\theta_{NO} - \theta_N \cos\theta_{NO}$$

$$\cos(\Phi_N - \Phi_H) = \cos(\phi_N + \phi_{NO} - \phi_H - \phi_{HO})$$
$$= \cos(\phi_{NO} - \phi_{HO})\cos(\phi_N - \phi_H)$$
$$- \sin(\phi_{NO} - \phi_{HO})\sin(\phi_N - \phi_H)$$
$$\approx \cos(\phi_{NO} - \phi_{HO})$$

$$\begin{aligned}
\sin(\Phi_N - \Phi_H) &= \sin(\phi_N + \phi_{NO} - \phi_H - \phi_{HO}) \\
&= \sin(\phi_{NO} - \phi_{HO}) \cos(\phi_N - \phi_H) \\
&\qquad - \cos(\phi_{NO} - \phi_{HO}) \sin(\phi_N - \phi_H) \\
&\approx \sin(\phi_{NO} - \phi_{HO})
\end{aligned}$$

The following approximations were also made to eliminate possible higher order terms:

$$\begin{aligned}
\cos\theta_N \cos\theta_H &= \cos(\theta_N + \theta_{NO}) \cos(\theta_H + \theta_{HO}) \\
&\approx \cos\theta_{NO} \cos\theta_{HO} - \theta_H \cos\theta_{NO} \sin\theta_{HO} \\
&\quad - \theta_N \sin\theta_{NO} \cos\theta_{HO} + \theta_N \theta_H \cos\theta_{NO} \sin\theta_{NO} \\
&\approx \cos\theta_{NO} \cos\theta_{HO}
\end{aligned}$$

$$\begin{aligned}
\cos\theta_N \sin\theta_H &= \cos(\theta_N + \theta_{NO}) \sin(\theta_H + \theta_{HO}) \\
&\approx \cos\theta_{NO} \sin\theta_{HO} + \theta_H \cos\theta_{NO} \sin\theta_{HO} \\
&\quad - \theta_N \sin\theta_{NO} \sin\theta_{HO} - \theta_N \theta_H \sin\theta_{NO} \cos\theta_{NO} \\
&\approx \cos\theta_{NO} \sin\theta_{HO}
\end{aligned}$$

$$\begin{aligned}
\sin\theta_N \sin\theta_H &= \sin(\theta_N + \theta_{NO}) \sin(\theta_H + \theta_{HO}) \\
&\approx \sin\theta_{NO} \sin\theta_{HO} + \theta_H \sin\theta_{NO} \cos\theta_{HO} \\
&\quad + \theta_N \cos\theta_{NO} \sin\theta_{HO} + \theta_N \theta_H \cos\theta_{NO} \cos\theta_{NO} \\
&\approx \sin\theta_{NO} \sin\theta_{HO}
\end{aligned}$$

Taking these approximations yields the final equation set:

$$\begin{aligned}
\theta_N : \quad & (m_N l_N^2 + m_H L_N^2 + I_{yy}^O)\ddot{\theta}_N - I_{yz}^O\ddot{\phi}_N \\
& + \{m_H L_N L_H\,[\cos\theta_{NO}\cos\theta_{HO}\cos(\phi_{NO}-\phi_{HO}) + \sin\theta_{NO}\sin\theta_{HO}]\}\ddot{\theta}_H \\
& + [m_H L_N L_H\,\cos\theta_{NO}\sin\theta_{HO}\sin(\phi_{NO}-\phi_{HO})]\ddot{\phi}_H \\
& + (\beta_{\theta N} + \beta_{\theta H})(\theta_N + \theta_{NO}) - \beta_{\theta H}(\theta_H + \theta_{HO}) \\
& + (m_N l_N + m_H L_N)\,[\ddot{x}\,\cos\theta_{NO}\cos\phi_{NO} + \ddot{y}\,\cos\theta_{NO}\sin\phi_{NO} \\
& - (\ddot{z} + g)(\sin\theta_{NO} + \theta_N\cos\theta_{NO}] = 0
\end{aligned}$$

$$\begin{aligned}
\phi_N : \quad & -I_{yz}^O\ddot{\theta}_N + [(m_N l_N^2 + m_H L_N^2)\sin^2\theta_{NO} + I_{zz}^O]\ddot{\phi}_N \\
& + [m_H L_N L_H\,\sin\theta_{NO}\cos\theta_{HO}\sin(\phi_{NO}-\phi_{HO})]\ddot{\theta}_H \\
& + [m_H L_N L_H\,\sin\theta_{NO}\sin\theta_{HO}\cos(\phi_{NO}-\phi_{HO})]\ddot{\phi}_H \\
& + (\beta_{\phi N} + \beta_{\phi H})(\phi_N + \phi_{NO}) - \beta_{\phi H}(\phi_H + \phi_{HO}) \\
& + (m_N l_N + m_H L_N)(-\ddot{x}\,\sin\theta_{NO}\sin\phi_{NO} + \ddot{y}\,\sin\theta_{NO}\cos\phi_{NO}) = 0
\end{aligned}$$

$$\begin{aligned}
\theta_H : \quad & \{m_H L_N L_H\,[\cos\theta_{NO}\cos\theta_{HO}\cos(\phi_{NO}-\phi_{HO}) + \sin\theta_{NO}\sin\theta_{HO}]\}\ddot{\theta}_N \\
& + [m_H L_N L_H\,\sin\theta_{NO}\cos\theta_{HO}\sin(\phi_{NO}-\phi_{HO})]\ddot{\phi}_N \\
& + (m_H L_H^2 + I_{yy}^P)\ddot{\theta}_H - I_{yz}^P\ddot{\phi}_H \\
& - \beta_{\theta H}(\theta_N + \theta_{NO}) + \beta_{\theta H}(\theta_H + \theta_{HO}) \\
& + m_H L_H\,[\ddot{x}\,\cos\theta_{HO}\cos\phi_{HO} + \ddot{y}\,\cos\theta_{HO}\sin\phi_{HO} \\
& \qquad - (\ddot{z} + g)(\sin\theta_{HO} + \theta_H\cos\theta_{HO})] = 0
\end{aligned}$$

$$\begin{aligned}
\phi_H : \quad & [m_H L_N L_H\,\cos\theta_{NO}\sin\theta_{HO}\sin(\phi_{NO}-\phi_{HO})]\ddot{\theta}_N \\
& + [m_H L_N L_H\,\sin\theta_{NO}\sin\theta_{HO}\cos(\phi_{NO}-\phi_{HO})]\ddot{\phi}_N \\
& - I_{yz}^P\ddot{\theta}_H - (m_H L_H^2\sin^2\theta_{HO} + I_{zz}^P)\ddot{\phi}_H \\
& - \beta_{\phi H}(\phi_N + \phi_{NO}) + \beta_{\phi H}(\phi_H + \phi_{HO}) \\
& + m_H L_H\,(-\ddot{x}\,\cos\theta_{HO}\cos\phi_{HO} + \ddot{y}\,\cos\theta_{HO}\sin\phi_{HO}) = 0
\end{aligned}$$

APPENDIX C

ONEEQ.FOR PROGRAM LISTING

```
C*********************************************************************
C
C                          ONEEQ.FOR
C
C    ONE DEGREE OF FREEDOM, Z DIRECTION IMPLEMENTATION
C    OF MATHEMATICAL MODEL FOR VARIABLE WEIGHT/CG HELMET
C    INVESTIGATION.  SOLVES FOR THETH AND PRODUCES
C    FREQUENCY RESPONSE INFORMATION FOR SINUSOIDAL
C    EXCITATION OVER A RANGE OF FREQUENCIES.
C
C*********************************************************************
C
      IMPLICIT REAL*8 (A-H,O-Z)
      REAL*8 LMDA5, LMDA4, IYYP, MH, LH
      INTEGER COUNT, FCOUNT
      DIMENSION FORCE(1024), QUAD(1024), IND6), XIND(2),
     &          XYMV(6), XYMV(6), ACV(1024), FREQ(1024),
     &          PS(1024), XCOV(1024), XSPECT(1024),
     &          AMPHAS(1024), XFER(1024), COHER(1024),
     &          QUAD2(1024), RESPN(1024)
C
C    INITIALIZE ARRAYS TO ZERO
C
10    TIME = 0.1D0
      DO 12 I = 1,1024
          FORCE(I) = 0.0D0
          QUAD(I) = 0.0D0
          ACV(I) = 0.0D0
          PS(I) = 0.0D0
          XCOV(I) = 0.0D0
          XSPECT(I) = 0.0D0
          AMPHAS(I) = 0.0D0
          XFER(I) = 0.0D0
          COHER(I) = 0.0D0
          QUAD2(I) = 0.0D0
          RESPN(I) = 0.0D0
12    CONTINUE
C*********************************************************************
C
C    ACQUIRE DATA FROM KEYBOARD INPUT
C
C              **********
C
      WRITE(6,100)
      WRITE(23,100)
100   FORMAT('WHAT IS THE COMBINED HEAD/HELMET MASS IN KG?')
```

```
      READ(5,*) MH
      WRITE(23,*) MH
C
      WRITE(6,105)
      WRITE(23,105)
105   FORMAT(' WHAT IS THE LENGTH OF THE HEAD ROD IN CM?')
      READ(5,*) LH
      WRITE(23,*) LH
C
      WRITE(6,110)
      WRITE(23,110)
110   FORMAT(' WHAT IS THE INITIAL ANGLE IN RADIANS?')
      READ(5,*) THETH0
      WRITE(23,*) THETH0
C
      WRITE(6,115)
      WRITE(23,115)
115   FORMAT(' WHAT IS IYY FOR THE COMBINED HEAD/HELMET',/,
     &        ' IN KG-CM**2 ?')
      READ(5,*) IYYP
      WRITE(23,*) IYYP
C
      WRITE(6,120)
      WRITE(23,120)
120   FORMAT(' WHAT IS THE SPRING CONSTANT IN N-CM/RAD ?')
      READ(5,*) BTHETH
      WRITE(23,*) BTHETH
C
      WRITE(6,125)
      WRITE(23,125)
125   FORMAT(' HOW MANY LINES OF FREQUENCY RESOLUTION?')
      READ(5,*) FCOUNT
      WRITE(23,*) FCOUNT
C
C
C*****************************************************************
C
C     DECLARE AND CALCULATE CONSTANTS
C
C              **********
C
      PI = 3.14159D0
      GRAV = 981.0D0             ! GRAVITY IN CM/SEC**2
C
      FMAX = 25.0D0              ! MAXIMUM FREQUENCY IN HZ
C
      ZAMP = 0.5D0*GRAV          ! AMPLITUDE IS 1G PEAK TO PEAK
C
      LMDA4 = MH*LH**2.0D0       ! MASS*LENGTH SCALARS FOR
      LMDA5 = MH*LH              ! OVERALL TORQUE CONCERNS
C
      A22 = LMDA4 + IYYP
```

```
      B22 = BTHETH - GRAV * LMDA5 * DCOS(THETH0)
C
      COUNT = 2 * FCOUNT        ! NUMBER OF T DOMAIN DATA PTS
      FSAMPLE = FMA*2.0D0       ! SAMPLE RATE
      DELTA = 1.0D0/FSAMPLE     ! TIME BETWEEN EACH SAMPLE
C
C**********************************************************
C
C     PROGRAM EXECUTION
C
C               **********
C
C     TIME DOMAIN CALCULATIONS
C
      WRITE(6,205)
      WRITE(23,205)
205   FORMAT(' TIME DOMAIN CALCULATIONS',/,/,'  TIME ',9X,
     &       '  FORCE ',8X,'  RESPONSE ',5X,'  ITERATION ')
C
          ISTART = FCOUNT/FMAX
      DO 505 J = ISTART, FCOUNT
C
          FF = DFLOAT(J)/DFLOAT(FCOUNT)*FMAX
C
               DO 500 I = 1,COUNT
C
                    OMG = FF*2.0D0*PI
                    OMG2 = OMG * OMG
                    OMGSIN = DSIN(OMG*TIME)
                    ROMGSIN = DSIN(OMG*TIME)
                    AMPZ = ZAMP/OMG2
C
C             FORCING FUNCTION
                    FORCE(I) = OMGSIN*AMPZ
C             SUMMATION OF FORCE
                    QUAD(I) = FORCE(I) + QUAD(I)
C
                    C2 = AMPZ*LMDA5*DSIN(THETH0)
                    BDENOM = B22/OMG2
                    ZDENOM = AMPZ*LMDA5*DCOS(THETH0)*OMGSIN
                    ENUME = C2*OMGSIN
                    DENOM = A22 - BDENOM + ZDENOM
C
C              RESPONSE FUNCTION
                    RESPN(I) = ENUME/(DENOM*OMGSIN)
C              SUMMATION OF RESPONSE
                    QUAD2(I) = RESPN(I) + QUAD2(I)
C
C
      WRITE(6,210) TIME, FORCE(I), RESPN(I), I
      WRITE(23,210) TIME, FORCE(I), RESPN(I), I
210   FORMAT(G13.6,2X,G13.6,2X,G13.6,5X,I4)
```

```
C
                 TIME = TIME + DELTA
C
500              CONTINUE
C
            TIME = 0.1D0
C
505         CONTINUE
C
      WRITE(6,220)
      WRITE(23,220)
220   FORMAT(' ',/,' TIME DATA CALCULATION COMPLETED',/,/)
C
C***********************************************************
C
C    FREQUENCY DOMAIN CALCULATIONS
C
C                **********
C
      IND(1) = 0                   ! INITIALIZE INDICATORS
      IND(2) = COUNT               ! FOR IMSL SUBROUTINE FTFREQ
      IND(3) = 1
      IND(4) = FCOUNT
      IND(5) = 0
      IND(6) = 0
C
      XIND(1) = DELTA
      XIND(2) = 0.0D0
C
C
      WRITE(6,225)
      WRITE(23,225)
225   FORMAT(' FREQUENCY DOMAIN CALCULATIONS',/,/)
C
C
C  ******   CALL IMSL SUBROUTINE FTFREQ   ******
C  ******   FORCING FUNCTION EVALUATION   ******
C
      CALL FTFREQ (QUAD,IND,XIND,XYMV,ACV,FREQ,PS,XCOV,
     &              XSPECT,AMPHAS,XFER,COHER,IER)
C
      WRITE(6,230) IER
      WRITE(23,230) IER
230   FORMAT(' FORCING FUNCTION OUTPUT   IER =  ',I5,/,/)
C
      WRITE(6,235)
      WRITE(23,235)
235   FORMAT(' STEP I ',5X,' PS(I) ',8X,' FREQ(I) ')
C
      DO 550 I = 1, FCOUNT+1
C
          WRITE(6,240) I, PS(I), FREQ(I)
```

```
          WRITE(23,240) I, PS(I), FREQ(I)
240       FORMAT(I5,5X,G13.6,2X,G13.6)
C
550   CONTINUE
C
C
      DO 560 I = 1,COUNT
C
          QUAD(I+COUNT) = QUAD2(I)
C
560   CONTINUE
C
      IND(1) = 1
C
C
C  ******   CALL IMSL SUBROUTINE FTFREQ   ******
C  ******   RESPONSE FUNCTION EVALUATION   ******
C
C
      CALL FTFREQ (QUAD,IND,XIND,XYMV,ACV,FREQ,PS,XCOV,
     &             XSPECT,AMPHAS,XFER,COHER,IER)
C
      WRITE(6,250) IER
      WRITE(23,250) IER
250   FORMAT(' RESPONSE FUNCTION OUTPUT   IER =  ',I5,/,/)
C
      WRITE(6,255)
      WRITE(23,255)
255   FORMAT(' FREQ ',7X,' XSPECT ',8X,' AMPHAS ',8X,
     &       ' PHASEANG ',6X,' COHER ')
C
      DO 570  I = 1,FCOUNT+1
          PHASANG = AMPHAS(I+FCOUNT) * 360.0D0
          IF(PHASANG.GT.180.0D0) PHASANG = PHASANG - 360.0D0
C
          WRITE(6,260) FREQ(I),XSPECT(I+FCOUNT),AMPHAS(I),
     &                 PHASANG,COHER(I)
          WRITE(23,260) FREQ(I),XSPECT(I+FCOUNT),AMPHAS(I),
     &                  PHASANG,COHER(I)
260       FORMAT(F10.4,2X,G13.6,2X,G13.6,2X,G13.6,2X,G13.6)
C
570   CONTINUE
C
C************************************************************
C
      WRITE(6,270)
      WRITE(23,270)
270   FORMAT(' END EXECUTION ')
C
      END
```

VITA

Christopher D. Hayes was born in Murfreesboro, Tennessee on September 30, 1959. In 1971, his family settled in Hermitage, Tennessee (a suburb of Nashville), where he attended DuPont Senior High School, graduating in June 1977.

An interest in science and biology lead to his enrollment in the Biomedical Engineering program at The University of Tennessee, Knoxville, where he graduated in August 1982 with a Bachelor of Science degree in Engineering Science and Mechanics. He enrolled in The Graduate School at the university that fall, accepting a Graduate Teaching Assistantship from the Engineering Science and Mechanics Department. His pursuit for the Master's degree in Engineering Science emphasized studies in dynamics and finite element analysis. His thesis research was performed under contract to the United States Army Aeromedical Research Laboratory at Fort Rucker, Alabama.

Mr. Hayes accepted a position with Sverdrup Technology, Inc. of Tullahoma, Tennessee in January 1986, where he is employed today as a Mechanical Design Engineer in Test Facility Design and Analysis.